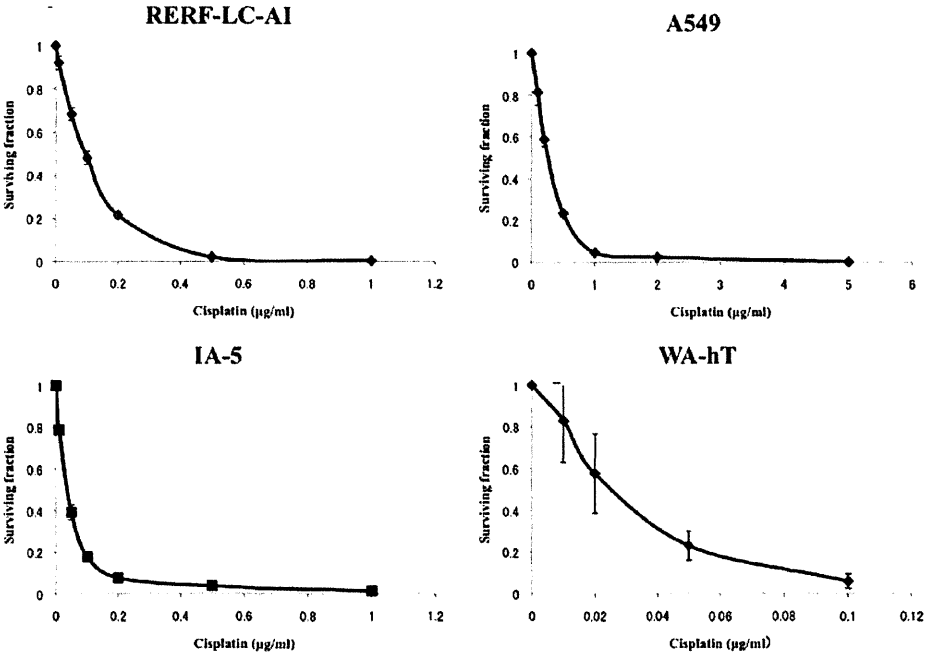


Figure 3. Survival curves drawn based on the results of the cell survival assay. The cells were treated with various concentrations of cisplatin instead of metformin. Other procedures were conducted as mentioned in Fig 2

there was no statistically significant difference except for the case of RERF-LC-AI, metformin induced G0/G1 phase accumulation in all 4 cell lines, whereas cisplatin at $IC_{70}$ caused significant G2/M phase accumulation in RERF-LC-AI and WA-hT, and G0/G1 phase accumulation in A549 cells. On the other hand, higher concentrations of cisplatin caused significant G2/M phase accumulation in all 4 cell lines (Fig. 5).

*Interaction of metformin and cisplatin.* In this experiment, cisplatin at $IC_{50}$ and $IC_{90}$ in each cell line was combined with metformin. The inhibitory effects of metformin on cell proliferation were slightly suppressed with cisplatin at $IC_{50}$ in all cells, except A549 cells. A higher dose ($IC_{90}$) of cisplatin almost completely countervailed or even reversed the effects of metformin in all cell lines except for A549, where a modest, but significant, sub-additive effect was observed (Fig. 6).

## Discussion

Metformin inhibited clonogenicity and cell proliferation in all 4 cell lines in a similar manner. On the other hand, WA-hT cells showed significantly higher sensitivity to cisplatin compared to the other cell lines. Concerning clonogenicity, the inhibitory effect of metformin was not specific to cancer cells because non-transformed mouse fibroblast and human mesothelial cell lines were also inhibited. Contrary to molecular targeted agents which specifically kill cancer cells harboring their specific targets, classical cytotoxic agents kill cells similarly even between cancer and non-transformed cells *in vitro* but preferably kill the former over the latter *in vivo* with differential effects to the cells according to different dividing capabilities. Therefore, it is speculated that metformin does not attack cancer-specific target molecules. In addition, the clonogenic assay disclosed that it is necessary to expose the cells to metformin for long periods of time to exert the inhibitory effects. As the surviving fraction reached a plateau in the range of 0.1-0.3 in the various cell lines with increasing doses of metformin (Fig. 2), the concentrations of $IC_{30}$ and $IC_{70}$ were chosen for further elucidating the mechanism of action.

Metformin did not enhance apoptosis at relatively low concentrations, as assessed by Hoechst staining and caspase activities in all cell lines except for WA-hT. Although the differences were not statistically significant except in RERF-LC-AI, metformin at $IC_{30}$ and $IC_{70}$ in each cell line tended to cause G0/G1 phase accumulation. Specifically, metformin exerted cytotoxicity by G0/G1 arrest in RERF-LC-AI, A549, and IA-5 and by both G0/G1 arrest and apoptosis in WA-hT cells. Although metformin may induce a different effect at higher concentrations, such high concentrations would not be clinically relevant. More specifically, the mean peak plasma concentration ($C_{max}$) in 5 Japanese diabetes patients was reportedly 0.85 ± 0.19 μg/ml ($5.1\pm1.1\times10^{-3}$ mM) when 250 mg of metformin was orally administered (21). Since the maximal single dose of 750 mg metformin is prescribed 3 times a day, an estimation of the $C_{max}$ would be $15\times10^{-3}$ mM. Although the dose range employed in the present research is approximately 100-fold higher than the plasma concentration that is achieved by conventional clinical application, the present results still seem clinically relevant for several reasons; a) chronic administration of metformin for months or even years in the clinical setting would be possible and the long-term exposure may augment its effects as demonstrated in Fig. 1; b) metformin accumulates in tissues at much higher concentrations than in the blood (22); and c) a dose-finding study for cancer treatment might determine the maximal tolerated dose of metformin at a much higher level than currently used for diabetic patients. Moreover, further elucidating the antiproliferative action of

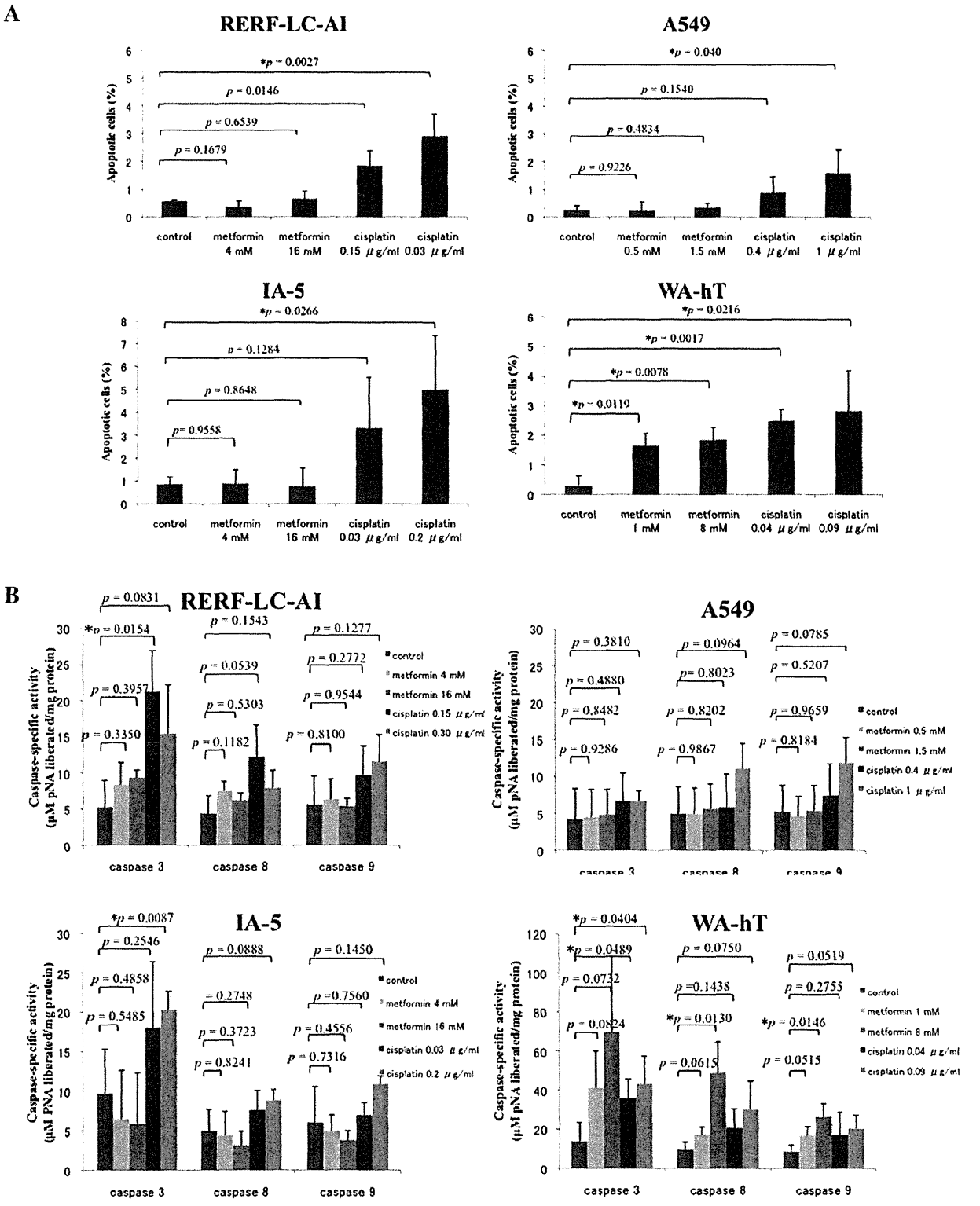


Figure 4. Apoptotic induction by treatment with metformin or cisplatin assessed by (A) Hoechst staining and (B) by caspase activities. The concentrations of metformin were $IC_{30}$ and $IC_{70}$ for each cell line. The concentrations of cisplatin were $IC_{70}$ and higher for each cell line. Differences from the control (no exposure to agents) were compared using the Student's t-test, and the resulting p-values are presented. *p<0.05 (two-tailed). Each experiment was repeated 3 times, and the mean ± SD values of the 3 experimental results are presented.

metformin may lead to the discovery of crucial target molecules for more effective new agents.

There is an increasing number of reports on the anti-neoplastic effects of metformin highlighting controversy in relation to its apoptotic induction and cell cycle alteration. Contrary to some studies reporting enhanced apoptosis in triple-negative breast cancer (6) and pancreatic cancer cells (10), others failed to observe apoptosis in non-triple-negative

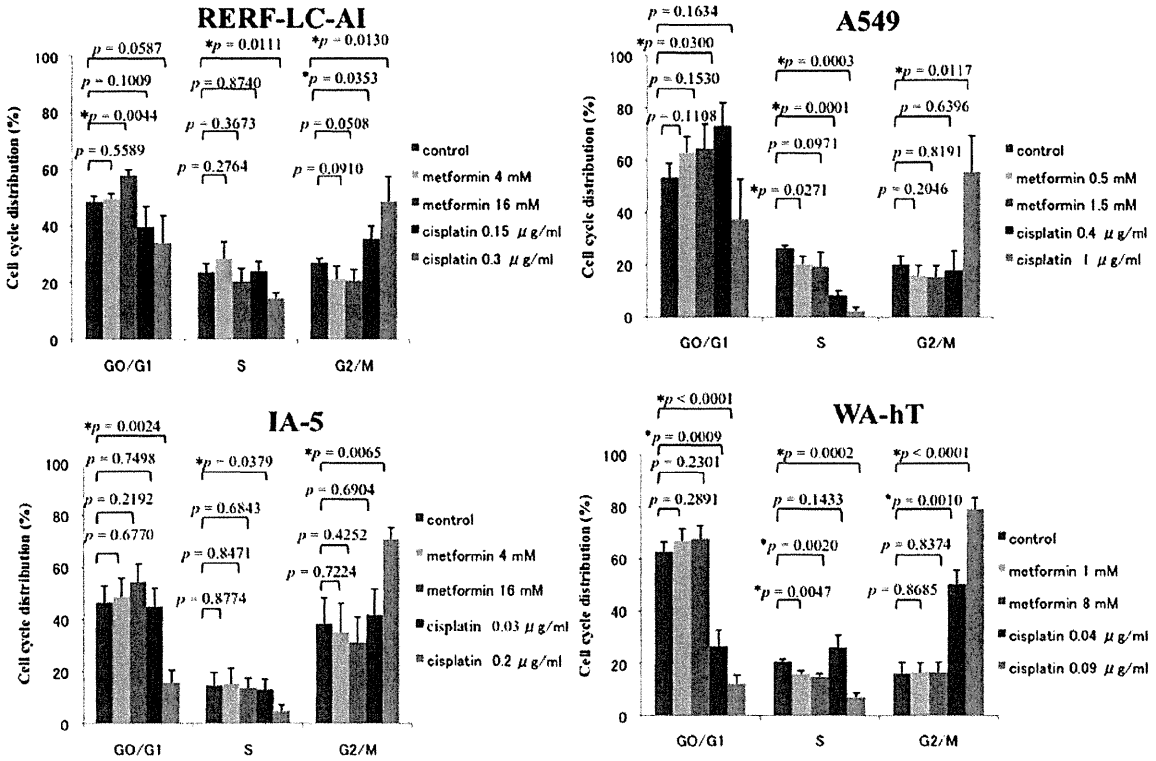


Figure 5. Alteration of cell cycle distribution by metformin or cisplatin assessed using the propidium iodide single-color method with a flow cytometer. Similarly to apoptosis analysis, the concentrations of metformin were $IC_{30}$ and $IC_{70}$ for each cell line, while the concentrations of cisplatin were $IC_{70}$ and higher for each cell line. Differences from the control (no exposure to agents) were compared using Student's t-test and the resulting p-values are presented. *p<0.05 (two-tailed). Each experiment was repeated 3 times, and the mean ± SD values of the 3 experimental results are presented.

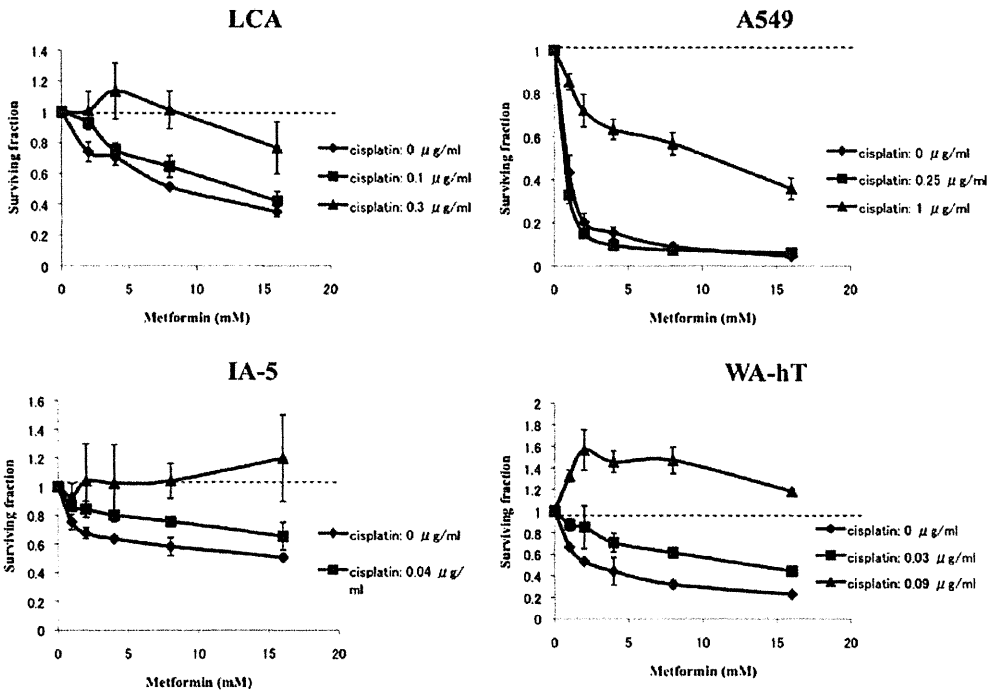


Figure 6. Interaction between metformin and cisplatin on cell proliferation inhibition. The cell survival assay was conducted using various concentrations of metformin as described in Fig. 2 except that the cells were exposed to 3 different concentrations of cisplatin, its $IC_{50}$ and $IC_{90}$ for each cell line and 0, together with metformin. In each curve with a defined cisplatin concentration, a fraction against the value without metformin was plotted at each metformin concentration point. Therefore, the curves located above the curve without cisplatin represent the antagonistic effects between the 2 agents. In particular, curves exceeding the line at fraction 1 (dotted lines) represent inverse effects, i.e., cell proliferation-enhancing effects by metformin treatment. Each experiment was conducted in triplicate and repeated 3 times. The mean value of each triplicate represents the value in each experiment, and the mean ± SD of the 3 experimental results were calculated. The dot and bar represent mean and SD at each point.

breast cancer (5) and a prostatic cancer cell line (9). Notably, cell cycle accumulation at the S phase was observed in a study on triple-negative breast cancer (6) and a pancreatic cancer cell line (10) that accompanied apoptosis enhancement, whereas an arrest at the G1 check point was observed in the non-triple-negative breast cancer (5) and the prostatic cancer cell line (9), and this arrest was not accompanied by apoptosis enhancement. In addition, G1 arrest was observed in an ovarian cancer cell line (12). The present results also differed among the cell lines, each of them representing a different histological type of human lung cancer. Metformin did not exert apoptosis induction but showed a tendency toward G0/G1 arrest in RERF-LC-AI, A549, and IA-5 cell lines, similarly to the results with non-triple-negative breast cancer (5) and prostatic cancer cell lines (9). However, WA-hT simultaneously underwent apoptosis and slight G0/G1 arrest. In view of the diversified results even among the 4 cell lines of a single disease, it would not be inappropriate to conclude that metformin affects different cancers or cancer cell lines differently.

The results of the combined effects of metformin and cisplatin are noteworthy. Administration of cisplatin at $IC_{50}$ along with metformin decreased the sensitivity to metformin in all 4 cell lines. Moreover, the combined use of metformin and high-dose cisplatin enhanced metformin-induced growth in all cell lines, excluding A549, because the cell survival curves of the other 3 cell lines exceeded the lines of fraction 1. Controversy exists in the literature with respect to the interaction with cisplatin. According to the research conducted by Gotlieb *et al* (11) and Rattan *et al* (13), metformin with cisplatin synergistically killed ovarian cancer cells. In contrast, Janjetovic *et al* (18) reported an antagonistic interaction between metformin and cisplatin in human glioma, rat glioma, human neuroblastoma, mouse fibrosarcoma, and human leukemia cell lines, possibly via an AMP kinase-independent upregulation of the Akt survival pathway. However, they also found augmented cisplatin sensitivity by metformin in a mouse melanoma cell line. Harhaji-Trajkovic *et al* (19) reported the antagonistic action of metformin on cisplatin. These findings again suggest that metformin affects different types of cancer, differently. On the other hand, the interaction between metformin and cisplatin in the present study was unexceptionally antagonistic in all 4 cell lines.

In conclusion, metformin inhibited the proliferation of various histological types of human lung cancer cell lines, possibly by varied mechanisms including apoptosis induction and G0/G1 arrest according to the cell line. Metformin and cisplatin were antagonistic in all 4 investigated cell lines. Taking account of its limited clinical adverse effects, metformin may have the potential for use in cancer therapy with adequate consideration of drug-drug interaction.

## Acknowledgements

This study was financially supported by a Grant-in-Aid for Scientific Research (grant no. 23591136) from the Japan Society for the Promotion of Science and the Ministry of Education, Culture, Sports, Science and Technology of Japan.

## References

1. Evans JM, Donnelly LA, Emslie-Smith AM, Alessi DR and Morris AD: Metformin and reduced risk of cancer in diabetic patients. BMJ 330: 1304-1305, 2005.
2. Bowker SL, Majumdar SR, Veugelers P and Johnson JA: Increased cancer-related mortality for patients with type 2 diabetes who use sulfonylureas or insulin. Diabetes Care 29: 254-258, 2006.
3. Jiralerspong S, Palla SL, Giordano SH, *et al*: Metformin and pathologic complete responses to neoadjuvant chemotherapy in diabetic patients with breast cancer. J Clin Oncol 27: 3297-3302, 2009.
4. Mazzone PJ, Rai HS, Beukemann M, Xu M, Abdallah R and Sasidhar M: The effect of metformin and thiazolidinedione use on lung cancer. Chest 138: 882A, 2010.
5. Alimova IN, Liu B, Fan Z, *et al*: Metformin inhibits breast cancer cell growth, colony formation and induces cell cycle arrest in vitro. Cell Cycle 8: 909-915, 2009.
6. Liu B, Fan Z, Edgerton SM, *et al*: Metformin induces unique biological and molecular responses in triple negative breast cancer cells. Cell Cycle 8: 2031-2040, 2009.
7. Zakikhani M, Dowling R, Fantus IG, Sonenberg N and Pollak M: Metformin is an AMP kinase-dependent growth inhibitor for breast cancer cells. Cancer Res 66: 10269-10273, 2006.
8. Rocha GZ, Dias MM, Ropelle ER, *et al*: Metformin amplifies chemotherapy-induced AMPK activation and antitumoral growth. Clin Cancer Res 17: 3993-4005, 2011.
9. Ben Sahra I, Laurent K, Loubat A, *et al*: The antidiabetic drug metformin exerts an antitumoral effect in vitro and in vivo through a decrease of cyclin D1 level. Oncogene 27: 3576-3586, 2008.
10. Wang LW, Li ZS, Zou DW, Jin ZD, Gao J and Xu GM: Metformin induces apoptosis of pancreatic cancer cells. World J Gastroenterol 14: 7192-7198, 2008.
11. Gotlieb WH, Saumet J, Beauchamp MC, *et al*: In vitro metformin anti-neoplastic activity in epithelial ovarian cancer. Gynecol Oncol 110: 246-250, 2008.
12. Rattan R, Giri S, Hartmann LC and Shridhar V: Metformin attenuates ovarian cancer cell growth in an AMP-kinase dispensable manner. J Cell Mol Med 15: 166-178, 2011.
13. Rattan R, Graham RP, Maguire JL, Giri S and Shridhar V: Metformin suppresses ovarian cancer growth and metastasis with enhancement of cisplatin cytotoxicity in vivo. Neoplasia 13: 483-491, 2011.
14. Pollak M: Insulin and insulin-like growth factor signalling in neoplasia. Nat Rev Cancer 8: 915-928, 2008.
15. Goodwin PJ, Ligibel JA and Stambolic V: Metformin in breast cancer: time for action. J Clin Oncol 27: 3271-3273, 2009.
16. Algire C, Zakikhani M, Blouin MJ, Shuai JH and Pollak M: Metformin attenuates the stimulatory effect of a high-energy diet on in vivo LLC1 carcinoma growth. Endocr Relat Cancer 15: 833-839, 2008.
17. Iliopoulos D, Hirsch HA and Struhl K: Metformin decreases the dose of chemotherapy for prolonging tumor remission in mouse xenografts involving multiple cancer cell types. Cancer Research 71: 3196-3201, 2011.
18. Janjetovic K, Vucicevic L, Misirkic M, *et al*: Metformin reduces cisplatin-mediated apoptotic death of cancer cells through AMPK-independent activation of Akt. Eur J Pharmacol 651: 41-50, 2011.
19. Harhaji-Trajkovic L, Vilimanovich U, Kravic-Stevovic T, Bumbasirevic V and Trajkovic V: AMPK-mediated autophagy inhibits apoptosis in cisplatin-treated tumour cells. J Cell Mol Med 13: 3644-3654, 2009.
20. Sugimoto T, Takiguchi Y, Kurosu K, *et al*: Growth factor-mediated interaction between tumor cells and stromal fibroblasts in an experimental model of human small-cell lung cancer. Oncol Rep 14: 823-830, 2005.
21. Iwase M, Nohara S, Sasaki N, *et al*: Pharmacokinetics study of low dose of metformin clinically used in Japan. J Japan Diab Soc 47: 197-201, 2004.
22. Wilcock C and Bailey CJ: Accumulation of metformin by tissues of the normal and diabetic mouse. Xenobiotica 24: 49-57, 1994.

Anjana | 10/16/12 | 4 color fig(s); F# | 01:57 | Art: JTO202259

ORIGINAL ARTICLE

# E1B-55 kDa-Defective Adenoviruses Activate p53 in Mesothelioma and Enhance Cytotoxicity of Anticancer Agents

AQ1 *Makako Yamanaka, MD,*‡ Yuji Tada, MD, PhD,‡ Kiyoko Kawamura, BS,* Quanhai Li, PhD,*§ Shinya Okamoto, PhD,¶ Kuan Chai, BS,*# Sana Yokoi, MD, PhD,† Min Liang, PhD,** Toshihiko Fukamachi, PhD,¶ Hiroshi Kobayashi, PhD,¶ Naoto Yamaguchi, PhD,# Atsushi Kitamura, MD,‡ Hideaki Shimada, MD, PhD,†† Kenzo Hiroshima, MD, PhD,‡‡ Yuichi Takiguchi, MD, PhD,‖ Koichiro Tatsumi, MD, PhD,‡ and Masatoshi Tagawa, MD, PhD*§*

**Introduction:** Genetic characterization of malignant mesothelioma shows a homozygous deletion of the INK4A/ARF locus, which results in inactivation of the p53 pathways.

**Methods:** We examined possible antitumor effects of adenoviruses with a deletion of the *E1B-55kD* gene (Ad-delE1B55) on mesothelioma and investigated combinatory actions with the first-line chemotherapeutic agents.

**Results:** Ad-delE1B55 produced cytotoxicity on mesothelioma cells, which was associated with p53 phosphorylation, pRb dephosphorylation, and cleavage of caspases. Ad-delE1B55–infected cells displayed hyperploidy at the cell-cycle analysis and showed enlarged nuclear configurations. Combination of Ad-delE1B55 plus cisplatin or pemetrexed produced antitumor effects in vitro. Furthermore, Ad-delE1B55 and cisplatin showed combinatory effects in an orthotopic animal model.

**Conclusions:** Cell death caused by Ad-delE1B55 is attributable to cell-cycle arrest at M-phase checkpoint followed by activated apoptotic pathways, and combination of the first-line chemotherapeutic agents and the oncolytic adenovirus is a potential therapeutic for mesothelioma.

AQ3 Divisions of *Pathology and Cell Therapy and †Translational Genomics, Chiba Cancer Center Research Institute, Chiba, Japan; Departments of ‡Respirology, §Molecular Biology and Oncology, and ‖Medical Oncology, Graduate School of Medicine, Chiba University, Chiba, Japan; Departments of ¶Biochemistry and #Molecular Cell Biology, Graduate School of Pharmaceutical Sciences, Chiba University, Chiba, Japan; AQ4 **TOT Shanghai RD Center, Shanghai, China; ††Department of Surgery, School of Medicine, Toho University, Tokyo, Japan; and ‡‡Department of Pathology, Tokyo Women's Medical University, Yachiyo Medical Center, Yachiyo, Japan.

AQ5 Disclosure: The authors declare no conflicts of interest.

Address for correspondence: Masatoshi Tagawa, MD, PhD, Division of Pathology and Cell Therapy, Chiba Cancer Center Research Institute, 666-2 Nitona, Chuo-ku, Chiba 260–8717, Japan. E-mail: mtagawa@chiba-cc.jp~~00002012~~



ISSN: 1556-0864/12/000-00

**Key Words:** Mesothelioma, Adenovirus, E1B-55 kDa, Chemotherapy, Hyperploidy.

(*J Thorac Oncol.* 2012;00:00-00)

Malignant mesothelioma, often associated with asbestos exposure, develops in the thoracic cavity. The latent period is beyond 30 years, and no preventive method after the exposure is currently available.[1] Early-stage patients can be subjected to radical surgical procedures, which nevertheless result in recurrence at a high frequency. Mesothelioma is resistant to radiotherapy and consequently chemotherapy is the primary treatment in most of the cases. A combination of cisplatin (CDDP) and pemetrexed (PEM) is currently the first-line regimen, but the average survival time with this combination is only 12.1 months.[2] The prognosis remains poor despite recent therapeutic modalities, and a novel strategy is required to improve the patient's quality of life.

Gene therapy is a possible strategy and has advantages in mesothelioma treatments. Mesothelioma in the pleural cavity is easily accessible for vectors, and consistent lung movements make the vectors spread into multiple sites. There have been several kinds of phase I clinical trials for mesothelioma with replication-deficient adenoviruses expressing either *herpes simplex-thymidine* kinase[3] or *interferon-ß* gene.[4] The trials confirmed safety of intrapleural Ad delivery, but these vectors transduced only a small fraction of the tumors. A vector system with enhanced efficacy is thereby preferable.

Replication-competent Ad continuously release the progenies from infected tumors and consequently circumvent low transduction efficacy. This replicable propensity enhances the cytotoxicity, although host immunity is inhibitory to the viral spreading. Ad lacking the E1B-55 kDa molecules (Ad-delE1B55) are replication competent and were originally hypothesized to target only *p53*-mutated or -null tumors because of the defect in p53-inactivating E1B-55 kDa protein.[5] However, subsequent studies showed that the replication was not linked with the *p53* genetic status.[6] Nevertheless,



<zjs;Original Article> • <zjss;XXX> • <zdoi;10.1097/JTO.0b013e3182725fa4>

Anjana | 10/16/12 | 4 color fig(s); F# | 01:57 | Art: JTO202259



Ad-delE1B55 demonstrated greater cytotoxicity to *p53*-mutated tumors than wild-type *p53* tumors.[7]

The majority of mesothelioma clinical specimens are defective of the INK4A/ARF locus containing the $p14^{ARF}$ and the $p16^{INK4A}$ genes but possess the wild-type *p53* gene.[8] Because $p14^{ARF}$ blocks Mdm2-mediated p53 degradation and $p16^{INK4A}$ inhibits cyclin-dependent kinases (CDK), the deletion results in loss of p53 functions and pRB phosphorylation, which subsequently leads to uncontrolled cell proliferation with enhanced resistance to apoptotic stimuli. Previous studies showed that forced expression of $p14^{ARF}$ or $p16^{INK4A}$ inhibited cell growth and induced apoptosis in mesothelioma.[9,10] Ad-delE1B55 can be a therapeutic agent in terms of the distinct genetic background of mesothelioma but has not been investigated for the cytotoxicity. In this study, we examined the Ad-delE1B55–mediated cytotoxicity with a panel of human mesothelioma cells and tested a possible combination with CDDP or PEM.

## MATERIALS AND METHODS

### Cells and Mice

Human mesothelioma, NCI-H2452, NCI-H2052, NCI-H226, NCI-H28, and MSTO-211H cells were cultured with RPMI 1640 medium with 10% fetal calf serum. BALB/c *nu/nu* mice were purchased from Japan SLC (Hamamatsu, Japan).

### Ad Preparation

Ad-delE1B55~~, in which the 55-kDa molecule encoding E1B region is deleted and replication incompetent~~ Ad expressing ß-*galactosidase* gene (Ad-LacZ) were prepared with an Adeno-X expression system (Takara, Shiga, Japan) with HEK293 cells.[11] Amounts of Ad were expressed as virus particles (vp*s*).

### In Vitro Cytotoxicity and Cell Proliferation

Cells ($5 \times 10^3$/well) in 96-well plates were cultured with Ad at different vp or chemotherapeutic agents. Cell viability was determined with a WST kit (Wako, Osaka, Japan), and the relative viability was calculated based on the absorbance without treatments. Viable cell numbers were counted with the trypan blue dye exclusion test. $IC_{50}$ values and combinatory effects were examined with CalcuSyn software (Biosoft, Cambridge, United Kingdom). Combination index (CI) values were calculated based on the cell viability and were shown with fractions affected (Fa) at respective doses. A CI value equal to 1 denotes an additive interaction, above 1 antagonism, and below 1 synergism.

### Western Blot Analysis

Cell lysate was subjected to sodium dodecyl sulfate polyacrylamide gel electrophoresis, and the protein was transferred to a nylon filter and then hybridized with antibody (Ab) against Ad E1A, Mdm2 (Santa Cruz Biotech, Santa Cruz, CA), Ad hexon, Mad2 (Abcam, Cambridge, United Kingdom), p53 (Lab vision, Fremont, CA), p27 (BD Biosciences, Franklin Lakes, NJ), caspase-3, cleaved caspase-3, caspase-8, caspase-9, phosphorylated-p53 at Ser 15 and Ser 46, p21, Fas, FADD, pRb, phosphorylated pRb (Cell Signaling, Danvers, MA), or actin (Sigma-Aldrich, St. Louis, MO) as a control. Anti–caspase-8 and anti–caspase-9 Ab detect respective cleaved molecules.

### Flow Cytometry and Cell Cycle

Cells were stained with anticoxsackie adenovirus receptor (CAR) antibody (Upstate Charlottesville, VA) and were analyzed with FACSCalibur and CellQuest software (BD, San Jose, CA). For cell-cycle analyses, adherent and nonadherent cells were collected after Ad infection, fixed in 100% ethanol, treated with RNase (50 µg/ml), and stained with propidium iodide (50 µg/ml). Cell-cycle distribution was analyzed with flow cytometry.

### Giemsa Staining and Apoptosis

Cells infected with Ad for 72 hours were treated with colcemid (10 ìg/ml), incubated with hypotonic buffer, and stained with Giemsa solution. These cells were examined for apoptosis with the TdT-mediated dUTP nick end-labeling method using an in situ cell-death detection kit (Roche Applied Science, Indianapolis, IN) followed by a nuclear staining with Kernechtrot solution (Muto Pure Chemicals, Tokyo, Japan).

### Animal Experiments

MSTO-211H cells ($1 \times 10^6$) were injected into the pleural cavity, and the mice received Ad intrapleurally and/or CDDP or phosphate-buffered saline intravenously as a control on day 3. The tumor weights were measured on day 29. The animal experiments were approved by the animal experiment and welfare committee at Chiba University and were performed according to the guideline on animal experiment.

## RESULTS

### Cytotoxicity of Ad-delE1B55

We examined cytotoxic activity of Ad-delE1B55 on mesothelioma cells, all of which are defective of the $p14^{ARF}$ and $p16^{INK4A}$ genes or of the corresponding transcriptions but possess the wild-type *p53* (Fig. 1A). All the cells, except NCI-H2052 cells, were susceptible to Ad-delE1B55 but not to Ad-LacZ. The expression level of CAR molecules, the major type 5 Ad receptor, was low in NCI-H2052 cells (Fig. 1*B*), which was partly linked with the insensitivity to Ad-delE1B55. $IC_{50}$ values based on the WST assay showed that NCI-H28 and MSTO-211H cells were most sensitive to Ad-delE1B55. We further examined proliferation kinetics of Ad-infected cells and demonstrated that numbers and viability of Ad-delE1B55–infected cells decreased after day 2, whereas uninfected or Ad-LacZ–treated cells did not (Fig. 2). These data suggested that Ad-delE1B55 infection induced growth arrest and cell death thereafter.

### Expression of p53-Linked and Apoptosis-Linked Protein

We examined expression levels of p53-linked protein in NCI-H28 cells after Ad-delE1B55 infection (Fig. 3A). Early

| Anjana | 10/16/12 | 4 color fig(s); F# | 01:57 | Art: JTO202259 |
|---|---|---|---|---|



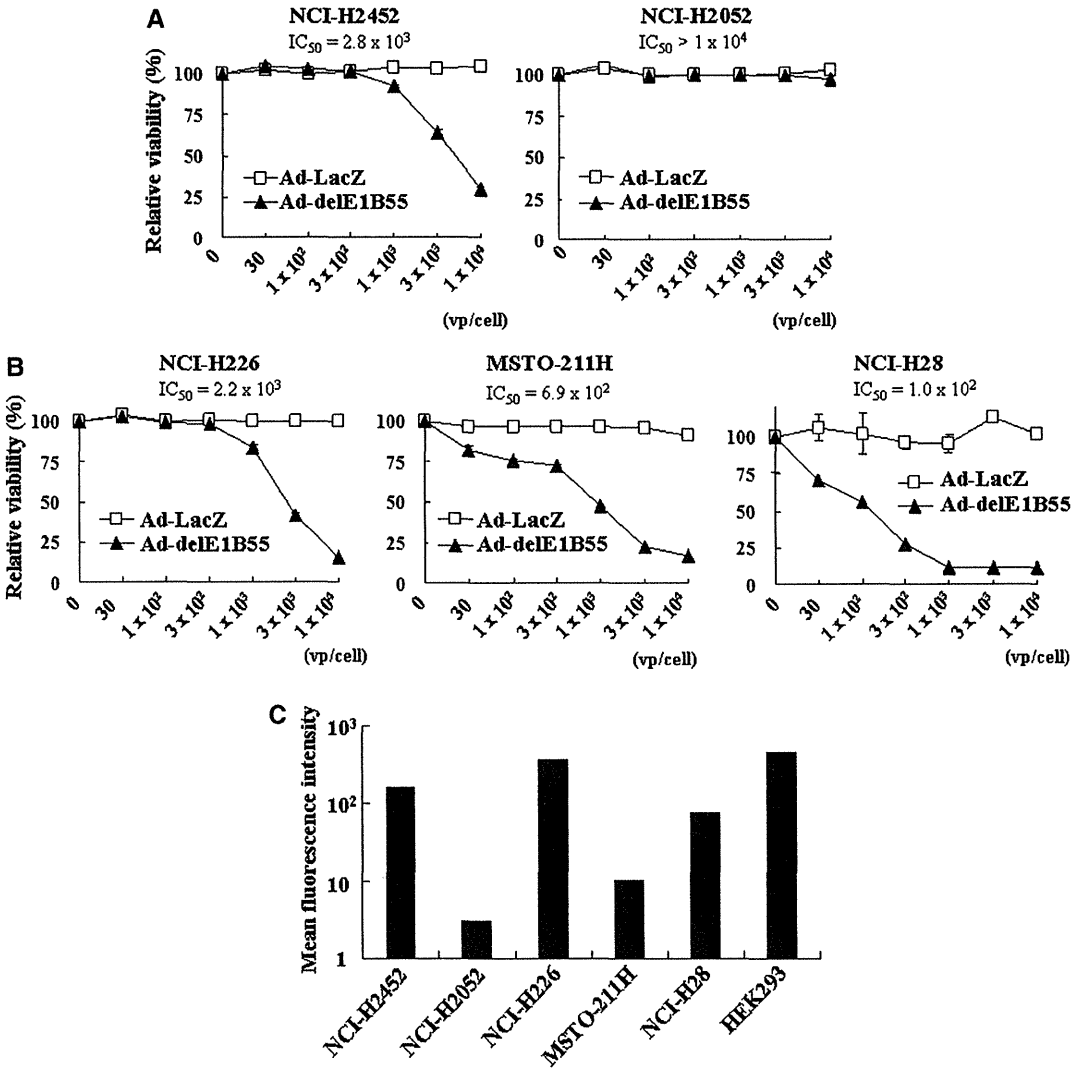


**FIGURE 1.** *A*, Cytotoxicity of Ad-delE1B55. Cells were infected with Ad-delE1B55 or Ad-LacZ, and the relative cell viability was calculated based on values of uninfected cells as 100%. SEs and $IC_{50}$ (vp/cell) of Ad-delE1B55 are also shown. *B*, Expression levels of CAR molecules analyzed with flow cytometry. The bar values showed mean fluorescence intensity expressed with an arbitrary FL1 unit. HEK293 cells were used for a standard.

viral E1A protein and late hexon protein became detectable at 24 and 48 hours after the infection, respectively. The infection up-regulated p53 expression levels and induced the phosphorylation at Ser 15 and then at 46 residues. Expression of cleaved 60 kDa Mdm2 moiety, which is a p53-binding form, was up-regulated but that of uncleaved 90 kDa Mdm2 was barely detected (data not shown). Anti-pRb Ab detected two bands corresponding to phosphoyrlated and dephosphorylated pRb, which migrated at high and low molecular weight, respectively, and probed the dephosphorylation more significantly in Ad-delE1B55–infected than in Ad-LacZ–infected cells. The decreased pRb phosphorylation was confirmed by antiphosphorylated pRb Ab. Expressions of CDK inhibitors, p21 and p27, were up-regulated in Ad-LacZ–infected cells but down-regulated in Ad-delE1B55–infected cells. Cells infected with Ad-LacZ became confluent with retarded growth under this experimental condition (Supplementary Figure 1, Supplementary Digital Content 1, http://links.lww.com/JTO/A342), which consequently induced dephosphorylated pRb and up-regulated CDK inhibitors. We examined expression levels of the p53-linked protein in Ad-infected MSTO-211H cells, and the results were similar to those in NCI-H28 cells (Fig. 3*C*). Up-regulated expressions of p53 and 60 kDa Mdm2, down-regulated expressions of pRb, phosphorylated pRB, p21, and p27, and cleavage of caspase-3 were also detected in MSTO-211H cells. Down-regulation of E1A and p53 phosphorylation was greater in MSTO-211H than in NCI-H28 cells.

We investigated possible apoptotic pathways, the extrinsic death receptor-mediated and the intrinsic mitochondria-mediated pathways (Fig. 3*B*). Both Ad-LacZ and Ad-delE1B55 infections increased caspase-8 expression,

 

Anjana | 10/16/12 | 4 color fig(s); F# | 01:57 | Art: JTO202259



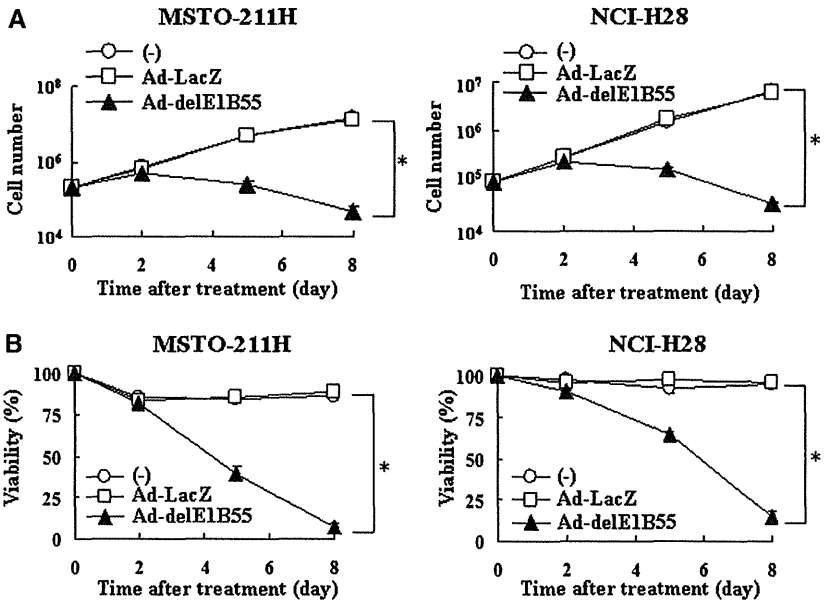


FIGURE 2. *A*, Cell proliferation and (*B*), viability of Ad-delE1B55–infected cells. NCI-H28 and MSTO-211H cells were infected with Ad (NCI-H28: $1 \times 10^3$, MSTO-211H: $4.5 \times 10^3$ vp/cell), and the cell numbers and the viability were determined with the trypan blue dye exclusion test. Cells reached at the confluence were seeded to keep cell growing. SEs are shown. *$p < 0.01$, compared with no treatment or Ad-LacZ group.

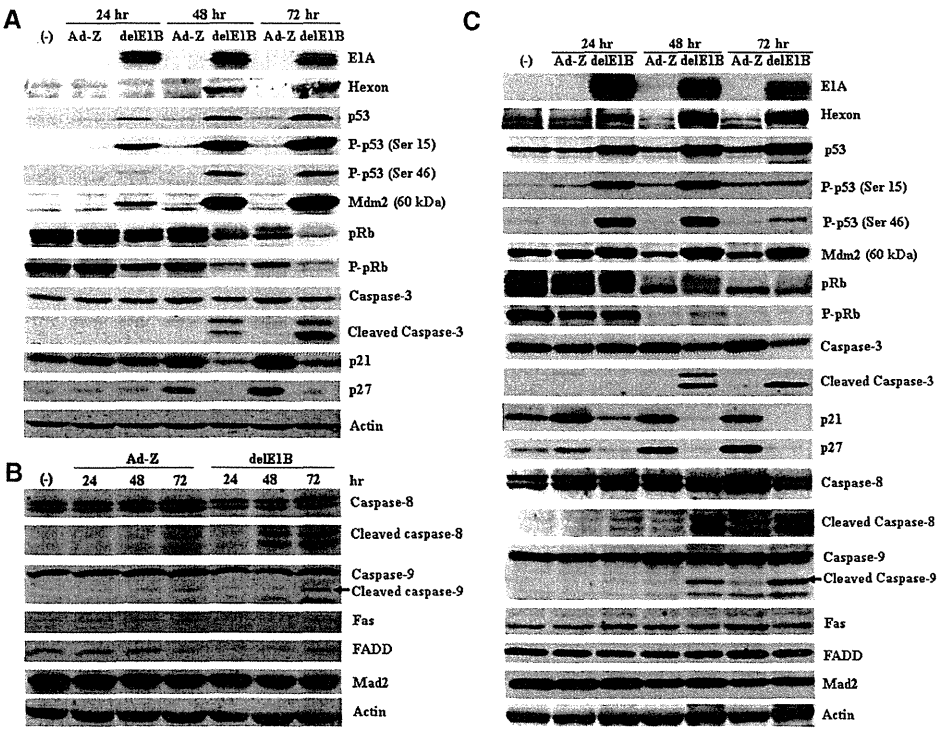


FIGURE 3. *A* and *B*, Ad-delE1B55–induced activation of p53 pathways. NCI-H28 and (C), MSTO-211H, cells were infected with Ad-delE1B55 (del-E1B) or Ad-LacZ (Ad-Z) at $1.5 \times 10^3$ vp/cell and cultured for the indicated times. Expression levels were analyzed with Western blot analyses. Actin was used as a control.

but cleaved caspase-8 was detected in Ad-delE1B55–infected cells. Cleavage of caspase-9 was less significant compared with that of caspase-8 but was found to be greater at the level in Ad-delE1B55–infected than in Ad-LacZ–infected cells. Expression levels of Fas and FADD, localized upstream to caspase-8 activation, remained unchanged by Ad infection. We also examined possible apoptotic pathways in MSTO-211H cells and detected the same expression patterns as found in NCI-H28 cells, except decreased Fas expression at 72 hours (Fig. 3*C*). We found that expression levels of the *BAX*, the *PUMA*, and the *NOXA* genes, linked with the intrinsic pathways, were not up-regulated by Ad-delE1B55 infection

Anjana | 10/16/12 | 4 color fig(s); F# | 01:57 | Art: JTO202259



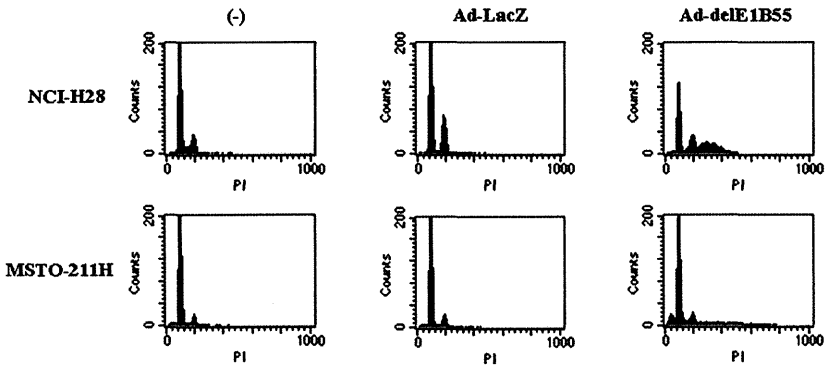


FIGURE 4. Representative profiles of cell-cycle analyses. Cells were treated with Ad-delE1B55 or Ad-LacZ (NCI-H28: $1 \times 10^3$, MSTO-211H: $4.5 \times 10^3$ vp/cell), or untreated for 72 hours.

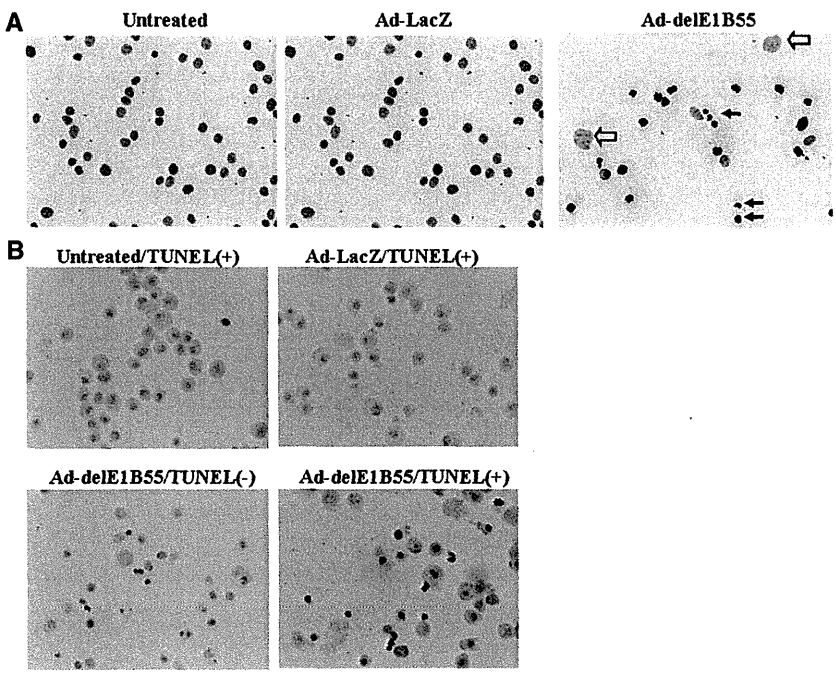


FIGURE 5. *A*, Nuclear morphological changes induced by Ad-delE1B55. NCI-H28 cells were infected with Ad ($1 \times 10^3$ vp/cell) followed by the Giemsa staining. In Ad-delE1B55–treated cells, small and highly condensed nuclei (solid arrow) and large and uncondensed nuclei (open) were detected. *B*, NCI-H28 cells infected with Ad ($1 \times 10^3$ vp/cell) were examined for apoptosis with the TUNEL assay and stained with Kernechtrot solution to visualize nuclei. TUNEL, terminal deoxynucleotidyl transferase–mediated deoxyuridine triphosphate-biotin nick end-labeling.

(data not shown). These data collectively suggested that Ad-delE1B55 induced caspase activations primarily through the extrinsic pathways, although the upstream pathways of caspase-8 remained unknown.

## Cell-Cycle Changes with Increased Hyperploidy

We investigated cell-cycle changes after Ad infection with NCI-H28 and MSTO-211H cells (Fig. 4; Table 1). Ad-LacZ infection induced minimal changes with slightly increased G2/M-phase fractions in NCI-H28 cells. Ad-delE1B55 infection gradually increased sub-G1 populations, which was notable in MSTO-211H cells. Before the increased sub-G1 fraction, a fraction with more than 4N populations (hyperploidy) increased in a time-dependent manner particularly in NCI-H28 cells. These results suggest that cells in the hyperploid fraction were subjected to apoptotic cell death.

We investigated whether the hyperploidy was attributable to any changes at a chromosomal level. We first examined chromosomal numbers at M-phase with colcemid treatment. NCI-H28 cells had increased chromosome numbers (average ± SE: 83.50±0.28), and the numbers remain unchanged after Ad-LacZ (84.86±0.44) or Ad-delE1B55 (85.50±0.42) infection. Constant chromosome numbers at M-phase can be because of a possibility that Ad-delE1B55–infected cells with hyperploid fractions did not enter into M-phase but stayed before G2-phase. We then examined any gene copy number changes with an array comparative genomic hybridization technique (Supplementary Figure 2, Supplementary Digital Content 2, http://links.lww.com/JTO/A343). Differential hybridization between Ad-delE1B55–infected and uninfected NCI-H28 or MSTO-211H cells did not reveal any gross chromosomal or gene copy number alternations. Furthermore, expression levels of Mad2, which inhibits chromosomal segregations in the spindle checkpoint, remained unchanged (Fig. 3*B* and 3*C*). We also examined nuclear morphology with the Giemsa staining method (Fig. 5A). Ad-delE1B55–infected cells demonstrated two characteristic patterns: an enlarged nuclear configuration and a small condensed nucleus, which were not detected in Ad-LacZ–infected cells.

Anjana | 10/16/12 | 4 color fig(s); F# | 01:57 | Art: JTO202259



We demonstrated that the cells with condensed nuclei were subjected to apoptosis (Fig. 5*B*). These data collectively suggested that Ad-delE1B55 infection increased nuclear DNA contents followed by pyknotic and apoptotic changes without gross chromosomal changes.

## Combinatory Effects

We investigated possible combinatory cytotoxic effects produced by Ad-delE1B55 and anticancer agents (Fig. 6). NCI-H28 and MSTO-211H cells were tested with different doses of CDDP or PEM to calculate $IC_{50}$ values (Fig. 6*A* and *C*). We then examined the susceptibility to Ad-delE1B55 in combination with the agents and calculated CI values at various Fa points. A combination of Ad-delE1B55 and CDDP produced synergistic effects in MSTO-211H cells at all the Fa points tested and either synergistic or additive effects in NCI-H28 cells at Fa below 0.75 (Fig. 6*B*). Ad-delE1B55 and PEM acted synergistically in NCI-H28 and MSTO-211H cells in the range of Fa 0.45 to 0.95 and Fa 0.65 to 0.95, respectively, and additive effects in lower Fa points (Fig. 6*D*). These results suggest that a combinatory use of Ad-delE1B55 and CDDP or PEM achieved synergistic cytotoxic effects in most cases of MSTO-211H cells and less significantly in NCI-H28 cells.

We also examined expression levels of p53 and the phosphorylation and caspase-3 cleavages in the combination (Fig. 6*E*). MSTO-211H cells treated with both Ad-delE1B and CDDP showed up-regulated p53 expression, p53 phosphorylation, and caspase-3 cleavage at a greater level than those treated with Ad-delE1B or CDDP. These data suggests that the combination augmented p53-mediated apoptotic processes. Cell-cycle analyses showed that the combinatory treatment increased sub-G1 populations greater than Ad-delE1B55 or CDDP treatment (Supplementary Table 1, Supplementary Digital Content 3, http://links.lww.com/JTO/A344). Interestingly, the combination amplified hyperploid fractions, but a role of CDDP in the enhanced hyperploidy is currently unknown.

## In Vivo Antitumor Effects

We investigated the antitumor effects of Ad-delE1B55 and a combinatory effect with CDDP in an orthotopic xenograft model (Table 2). Ad-delE1B55 administration did not produce the antitumor effects at a low dose ($1 \times 10^{10}$ vp) but achieved the effects at a high dose ($8 \times 10^{10}$ vp). Tumor growth of the mice treated with Ad-delE1B55 ($1 \times 10^{10}$ vp) plus CDDP was more inhibited than that of the group treated with either Ad-delE1B55 or CDDP. The high-dose Ad-delE1B55 suppressed the tumor growth to a great extent, and consequently the combination effects with CDDP were not detected with statistical significance, although the combination produced better therapeutic effects than CDDP alone. In contrast, Ad-LacZ did not achieve antitumor effects or the combinatory effects. An intermediate Ad dose ($3 \times 10^{10}$ and $6 \times 10^{10}$ vp) produced combinatory effects with CDDP (Supplementary Table 2, Supplementary Digital Content 4, http://links.lww.com/JTO/A345). Mice body weights were not retarded by Ad administration, suggesting that mice tolerated intrapleural Ad injections.

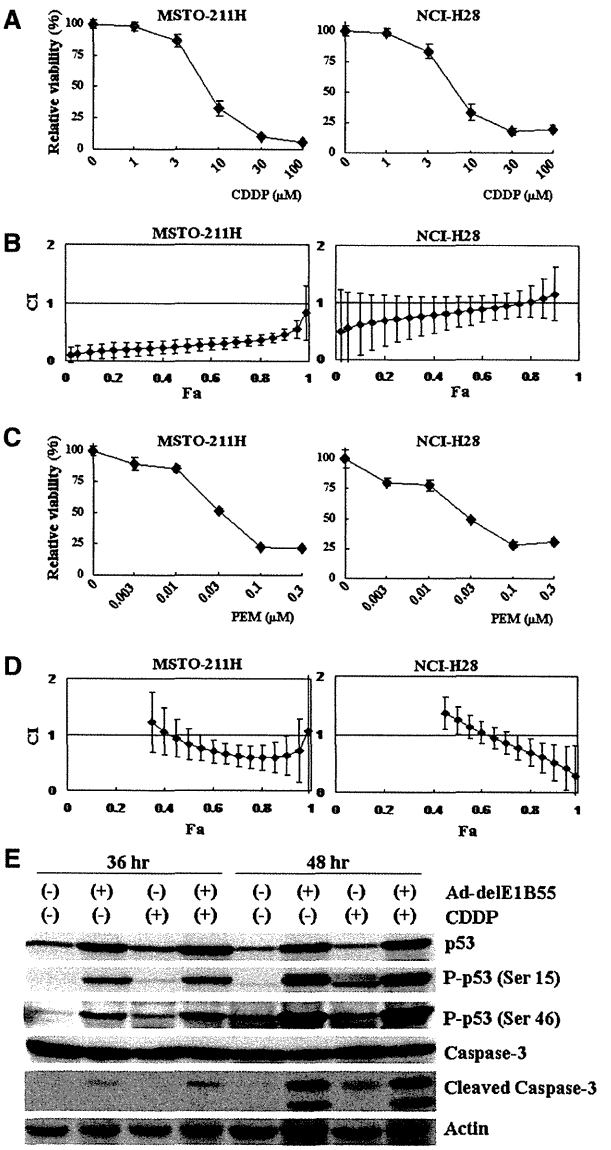


F6

FIGURE 6. *A*, Combinatory effects of Ad-delE1B55 and CDDP or PEM. Cells were treated with different doses of CDDP or (*C*) PEM , and the relative cell viabilities were calculated based on values of untreated cells as 100%. *B*, Cells were also treated with various vp of Ad-delE1B55 and concentrations of CDDP or (*D*), PEM . CIs were calculated with CalcuSyn software and plotted in respective Fa points. SEs are shown. *E*, MSTO-211H cells were treated with Ad-delE1B55 ($1.5 \times 10^3$ vp/cell) and/or with CDDP (10 μM). Expression levels of the indicated proteins were analyzed with Western blot analyses. Actin was used as a control. CDDP, cis-diamminedichloroplatinum; PEM, pemetrexed.

T2

## DISCUSSION

To our knowledge, our study demonstrated the cytotoxicity of Ad-delE1B55 to p14/p16-defective mesothelioma. Ad-delE1B55 up-regulated p53 probably through viral E1A and phosphorylated p53 at Ser 15 and 46 residues, both of

Anjana | 10/16/12 | 4 color fig(s); F# | 01:57 | Art: JTO202259



**TABLE 1.** Cell-Cycle Distribution after Ad Infection

| Cells | Time (hr) | Treatment[a] | Cell-Cycle Distribution (%±SE)[b] | | | | |
|---|---|---|---|---|---|---|---|
| | | | Sub-G1 | G1 | S | G2/M | >4N |
| NCI-H28 | 24 | (—) | 0.15±0.03 | 65.00±3.14 | 18.33±0.74 | 16.81±2.34 | 0.24±0.09 |
| | | Ad-LacZ | 0.14±0.04 | 56.52±0.22 | 18.31±0.33 | 24.83±0.19 | 0.57±0.10 |
| | | Ad-delE1B55 | 0.17±0.04 | 63.52±0.43 | 16.47±0.10 | 18.11±0.54 | 2.07±0.09[c] |
| | 48 | (—) | 0.13±0.04 | 65.94±0.23 | 14.75±0.09 | 18.61±0.15 | 0.90±0.06 |
| | | Ad-LacZ | 0.23±0.05 | 62.44±0.50 | 8.35±0.07 | 27.37±0.53 | 1.83±0.13 |
| | | Ad-delE1B55 | 0.61±0.08[c] | 28.14±0.00 | 17.23±0.56 | 24.28±0.45 | 30.25±0.05[c] |
| | 72 | (—) | 0.13±0.03 | 75.55±0.22 | 9.71±0.28 | 13.44±0.45 | 1.15±0.04 |
| | | Ad-LacZ | 0.25±0.02 | 71.07±0.04 | 3.25±0.08 | 24.11±0.30 | 1.51±0.20 |
| | | Ad-delE1B55 | 1.09±0.05[c] | 30.87±0.28 | 6.19±0.19 | 13.94±0.08 | 48.21±0.44[c] |
| MSTO-211H | 24 | (—) | 1.27±0.03 | 61.78±0.74 | 13.62±0.32 | 21.85±0.27 | 1.48±0.16 |
| | | Ad-LacZ | 1.37±0.09 | 60.33±0.40 | 14.66±0.26 | 22.37±0.34 | 1.46±0.05 |
| | | Ad-delE1B55 | 1.37±0.05 | 62.67±0.45 | 12.47±0.10 | 21.33±0.32 | 2.24±0.14[c] |
| | 48 | (—) | 0.66±0.06 | 79.43±0.45 | 6.61±0.24 | 12.70±0.53 | 0.72±0.02 |
| | | Ad-LacZ | 1.05±0.04 | 79.11±0.27 | 5.51±0.19 | 13.26±0.06 | 1.19±0.04 |
| | | Ad-delE1B55 | 3.70±0.12[c] | 68.77±0.65 | 6.95±0.15 | 13.25±0.28 | 7.53±0.45[c] |
| | 72 | (—) | 2.15±0.05 | 89.09±0.13 | 1.82±0.10 | 6.45±0.06 | 0.61±0.04 |
| | | Ad-LacZ | 2.39±0.18 | 87.21±0.26 | 1.84±0.05 | 7.99±0.09 | 0.65±0.07 |
| | | Ad-delE1B55 | 10.13±0.42[c] | 57.31±0.60 | 5.95±0.24 | 9.33±0.28 | 17.76±0.38[c] |

[a] Cells were infected with Ad-LacZ or Ad-delE1B55 (H28: $1 \times 10^3$, 211H: $4.5 \times 10^3$ vp/cell) and cultured for 24 to 72 hr.
[b] ~~Cell-cycle~~ profiles were analyzed with flow cytometry. Mean percentages with SEs are shown ($n = 3$).
[c] $p < 0.01$, compared with no treatment or Ad-LacZ group.
AD, adenovirus;

**TABLE 2.** Effects of Ad-delE1B55 and CDDP on Mesothelioma in Nude Mice

| | Ad (vp/mouse) Treatment[a] | Tumor Weight (mg) (average ± SE)[b] | |
|---|---|---|---|
| | | CDDP (−)[a] | CDDP (+)[a] |
| Exp 1 | (—) | 273±23[1] | 149±22[1,4] |
| | Ad-LacZ ($1 \times 10^{10}$) | 271±34[2] | 124±9[2] |
| | Ad-delE1B ($1 \times 10^{10}$) | 225±52[3] | 47±13[3,4] |
| Exp 2 | (—) | 278±44[5] | 112±28[5,8] |
| | Ad-LacZ ($8 \times 10^{10}$) | 244±10[6,7] | 76±30[6,9] |
| | Ad-delE1B ($8 \times 10^{10}$) | 22±8[7] | 4±1[8,9] |

[a] Mice were injected with MSTO-211H ($1 \times 10^6$) into the pleural cavity (day 1) and were treated with intrapleural Ad (day 3) and/or intraperitoneal CDDP (0.12 mg/mouse) administrations (day 3). PBS was also injected as a control in Ad (−) or CDDP (−) groups.
[b] Tumor weight was measured on day 29. Average with SEs are shown ($n = 6$–7). $p < 0.01$,[1-3,5-8] $p < 0.05$.[4,9]
Ad, adenovirus; CDDP, cis-diamminedichloroplatinum.

AQ8

which are linked with cell-cycle arrest and apoptosis, respectively. The mechanism for p53 phosphorylation without DNA damages is currently unknown, but the viral replication itself may induce the phosphorylation because Ad-LacZ did not phosphorylate endogenous p53. Cleaved 60 kDa Mdm2 binds to p53 and inhibits degradation, which can contribute to the p53 upregulation.[12] We scarcely detected the full-length 90 kDa molecules despite an assumption that the full-length molecules can be overexpressed as a result of deficit of Mdm2-inhibiting p14. Activation of p53 pathways by Ad-delE1B55 did not augment p21 expression. Increased p21 was inhibitory to cell death, and decreased p21 rather promoted Ad replication and cell death.[13] CDK expressions were thus not directly linked with p53 activation. The down-regulated CDK expressions were also associated with decreased pRb phosphorylation, which inhibits cell-cycle progression into S-phase. These data collectively suggest that Ad-delE1B55 restored p53 and pRb functions as a tumor suppressor.

Ad-delE1B55 induced cell death, which was evidenced by increased sub-G1 fraction and loss of viability. Caspase-3 and caspase-8 were cleaved, but caspase-9 cleavage was less significant. Moreover, transcription of the *Puma*, the *Noxa*, and the *BAX* genes did not increase (data not shown). These data indicated that the cell death was induced primarily by the extrinsic pathways and involvement of the intrinsic pathway was relatively minor. Expression levels of Fas and FADD remain unchanged, and the upstream signaling of the extrinsic pathways needs further investigations. Moreover, our preliminary data showed that expression levels of some autophagy markers such as Atg5 remained unchanged after Ad-delE1B55 infection, suggesting that involvement of autophagy was less likely in cell death.

Flow cytometrical analyses demonstrated increase of hyperploid populations followed by augmented sub-G1 fractions. Cherubini et al.[14] showed that Ad-delE1B55 induced hyperlploidy in the *p53* wild-type nontumorous cells and demonstrated increased expression of Mad2, a major component of M-phase checkpoint. The study indicated that wild-type Ad did not induce hyperploidy, eliminating a possibility that hyperploidy was caused by amplified viral

 

Anjana | 10/16/12 | 4 color fig(s); F# | 01:57 | Art: JTO202259



DNA. Our preliminary data also showed that the wild-type Ad minimally induced hyperploidy and rapidly increased sub-G1 fractions. The current study showed that Mad2 expression and chromosomal numbers at M-phase remained unchanged. We thereby speculate that Ad-delE1B55–infected cells could not enter into M-phase and the cell cycle stopped before G2 checkpoint. Aberrant mitosis is known to lead to cell death, and the morphological characteristics such as enlarged and multinucleated cells are hallmarks of the mitotic catastrophe.[15] The current data instead showed that cells with enlarged and condensed nuclei became apoptotic, and array comparative genomic hybridization data excluded possible amplified chromosomal regions. A molecular basis of the Ad-induced hyperploidy is therefore currently unknown.

We demonstrated combinatory effects of Ad-delE1B55 and CDDP or PEM. Anticancer agents can suppress viral replication by inhibiting protein synthesis in host cells, but our previous study demonstrated that it was not always the case.[11] Ad-delE1B55 infection increased susceptibility of mesothelioma to CDDP and to a lesser extent to PEM. The differential effect of Ad-delE1B55 may be linked with up-regulated p53 expression and pRb dephosphorylation. Up-regulated p53 resulted in enhanced sensitivity to anticancer agents by augmenting apoptotic pathways.[16] The current study demonstrated that the combinatory use of Ad-delE1B55 and CDDP induced p53 phosphoylation and caspase-3 cleavage greater than each agent alone. Ad-delE1B55 also inhibited cell-cycle progression through pRb dephosphorylation, which decreases effects of agents inhibiting DNA replication. PEM, inhibiting DNA synthesis, is thus less effective compared with CDDP.

We demonstrated combinatory effects of Ad-delE1B55 and CDDP in an orthotopic model, which suggests clinical feasibility. Mesothelioma patients often have pleural effusion, and the tumors extend along the thoracic cavity. Intrapleural injection makes Ad spread the cavity lining and increased the infectivity. Moreover, pleural administration has less chance of hepatotoxicity, the major Ad toxicity, because of multiple barriers for Ad to spread into liver. The current study however suggested that low CAR-expressing mesothelioma could be resistant to Ad-mediated cytotoxicity.

In summary, the current study demonstrated that Ad-delE1B55 was a possible agent for mesothelioma through activating p53 pathways and produced combinatory antitumor effects with the first-line chemotherapeutic agents currently used.

## ACKNOWLEDGMENTS

*Supported by grants-in-aid for scientific research from the Ministry of Education, Culture, Sports, Science and Technology of Japan, for Cancer Research from the Ministry of Health, Labor and Welfare of Japan, and a grant-in-aid from the Nichias Corporation and the Futaba Electronics Memorial Foundation.*

## REFERENCES

1. Robinson BW, Musk AW, Lake RA. Malignant mesothelioma. *Lancet* 2005;366:397–408.
2. Vogelzang NJ, Rusthoven JJ, Symanowski J, et al. Phase III study of pemetrexed in combination with cisplatin versus cisplatin alone in patients with malignant pleural mesothelioma. *J Clin Oncol* 2003;21:2636–2644.
3. Sterman DH, Recio A, Vachani A, et al. Long-term follow-up of patients with malignant pleural mesothelioma receiving high-dose adenovirus herpes simplex thymidine kinase/ganciclovir suicide gene therapy. *Clin Cancer Res* 2005;11:7444–7453.
4. Sterman DH, Recio A, Haas AR, et al. A phase I trial of repeated intrapleural adenoviral-mediated interferon-beta gene transfer for mesothelioma and metastatic pleural effusions. *Mol Ther* 2010;18:852–860.
5. Bischoff JR, Kirn DH, Williams A, et al. An adenovirus mutant that replicates selectively in p53-deficient human tumor cells. *Science* 1996;274:373–376.
6. Rothmann T, Hengstermann A, Whitaker NJ, Scheffner M, zur Hausen H. Replication of ONYX-015, a potential anticancer adenovirus, is independent of p53 status in tumor cells. *J Virol* 1998;72:9470–9478.
7. You L, Yang CT, Jablons DM. ONYX-015 works synergistically with chemotherapy in lung cancer cell lines and primary cultures freshly made from lung cancer patients. *Cancer Res* 2000;60:1009–1013.
8. Lee AY, Raz DJ, He B, Jablons DM. Update on the molecular biology of malignant mesothelioma. *Cancer* 2007;109:1454–1461.
9. Yang CT, You L, Yeh CC, et al. Adenovirus-mediated p14(ARF) gene transfer in human mesothelioma cells. *J Natl Cancer Inst* 2000;92:636–641.
10. Frizelle SP, Grim J, Zhou J, et al. Re-expression of p16INK4a in mesothelioma cells results in cell cycle arrest, cell death, tumor suppression and tumor regression. *Oncogene* 1998;16:3087–3095.
11. Ma G, Kawamura K, Li Q, et al. Combinatory cytotoxic effects produced by E1B-55kDa-deleted adenoviruses and chemotherapeutic agents are dependent on the agents in esophageal carcinoma. *Cancer Gene Ther* 2010;17:803–813.
12. Pochampally R, Fodera B, Chen L, Lu W, Chen J. Activation of an MDM2-specific caspase by p53 in the absence of apoptosis. *J Biol Chem* 1999;274:15271–15277.
13. Shiina M, Lacher MD, Christian C, Korn WM. RNA interference-mediated knockdown of p21(WAF1) enhances anti-tumor cell activity of oncolytic adenoviruses. *Cancer Gene Ther* 2009;16:810–819.
14. Cherubini G, Petouchoff T, Grossi M, Piersanti S, Cundari E, Saggio I. E1B55K-deleted adenovirus (ONYX-015) overrides G1/S and G2/M checkpoints and causes mitotic catastrophe and endoreduplication in p53-proficient normal cells. *Cell Cycle* 2006;5:2244–2252.
15. de Bruin EC, Medema JP. Apoptosis and non-apoptotic deaths in cancer development and treatment response. *Cancer Treat Rev* 2008;34:737–749.
16. Roth JA. Adenovirus p53 gene therapy. *Expert Opin Biol Ther* 2006;6:55–61.

# AUTHOR QUERIES

## AUTHOR PLEASE ANSWER ALL QUERIES

AQ1—Please confirm that all author names are correct and appear with the given name first, followed by the surname.

AQ2—Please provide departmental names for authors Makako Yamanaka, Quanhai Li, Kuan Chai, Sana Yokoi, Masatoshi Tagawa, Kiyoko Kawamura.

AQ3—

AQ4—Please provide departmental name and division for author, Min Liang.

AQ5—Please verify the statement of conflict.

AQ6—Please provide expansion of RPMI, if appropriate.

AQ7—Please rewrite for clarity the sentence beginning with "Ad-delE1B55, in which...."

AQ8—Please provide the expansion of PBS.

AQ9—Please review the edits to the sentence beginning with "To our knowledge..."

International Journal of Cardiology 159 (2012) 119–127

Contents lists available at ScienceDirect

International Journal of Cardiology

journal homepage: www.elsevier.com/locate/ijcard

# Characterization of myofibroblasts in chronic thromboembolic pulmonary hypertension

Miki Maruoka [a,*,1], Seiichiro Sakao [a,1], Masashi Kantake [a], Nobuhiro Tanabe [a], Yasunori Kasahara [a], Katsushi Kurosu [a], Yuichi Takiguchi [a], Masahisa Masuda [b], Ichiro Yoshino [c], Norbert F. Voelkel [d], Koichiro Tatsumi [a]

[a] Department of Respirology, Graduate School of Medicine, Chiba University, 1-8-1 Inohana, Chuo-ku, Chiba 260-8670, Japan
[b] Chiba Medical Center, National Hospital Organization, 4-1-2 Tubakimori, Chuo-ku, Chiba 260-8606, Japan
[c] Department of Thoracic Surgery, Graduate School of Medicine, Chiba University, 1-8-1 Inohana, Chuo-ku, Chiba 260-8670, Japan
[d] Victoria Johnson Center for Obstructive Lung Diseases, Virginia Commonwealth University, 1101 East Marshall Street, Sanger Hall, Richmond, VA 23298-0565, USA

ARTICLE INFO

*Article history:*
Received 25 August 2010
Received in revised form 2 February 2011
Accepted 10 February 2011
Available online 15 March 2011

*Keywords:*
Pulmonary circulation
Pulmonary hypertension
Pulmonary thromboembolism

ABSTRACT

*Background:* It has been generally accepted that chronic thromboembolic pulmonary hypertension (CTEPH) results from pulmonary embolism arising from deep vein thrombosis. An unresolved question regarding the etiology of CTEPH is why pulmonary thromboemboli are stable and resistant to effective anticoagulation. Recently non-resolving pulmonary thromboemboli in CTEPH have been shown to include myofibroblasts. This study investigates the cellular characteristics of myofibroblasts included in the organized thrombotic tissues of CTEPH.

*Methods:* Organized thrombotic tissues of patients with CTEPH were obtained following pulmonary endarterectomy. We isolated cells from endarterectomized tissue from patients with CTEPH and identified them as endothelial-like cells and myofibroblast-like cells.

*Results:* Myofibroblast-like cells were characterized as hyperproliferative, anchorage-independent, invasive and serum-independent.

*Conclusions:* Here we report the presence of active myofibroblast-like cells in endarterectomized tissue of CTEPH. We suggest that the formation of myofibroblasts with a high growth potential in the organized thrombotic tissues may be an important event in the pathobiology of this disease.



## 1. Introduction

It is generally accepted that chronic thromboembolic pulmonary hypertension (CTEPH) results from pulmonary embolism originating from deep vein thrombosis [1,2]. Based on recent insights, however, this mechanistic view of CTEPH may have been too simplistic [3,4].

It is becoming increasingly acknowledged that although central thrombi are the most likely disease-initiating event, progressive small-vessel disease may contribute to the long-term progression of pulmonary hypertension (PH) [4–7]. Studies also suggest that *in situ* thrombosis in the lung may contribute to disease progression, promoting the stabilization and growth of thromboemboli [3,4].

Pulmonary endaretectomy (PEA) is the current mainstay of therapy for patients with CTEPH. The aim of PEA is the removal of organized and incorporated fibrous obstructive tissue from the pulmonary arterial tree as completely as possible while avoiding pulmonary vascular injury. Although small-vessel disease may develop during the course of CTEPH, it is uncertain whether PEA has a beneficial effect on the disease that is established at the time of surgery [8]. After the successful treatment of PEA, the right ventricle recovers and maintains normal function over time, regardless of the severity of preoperative disease. However, the effect of residual pulmonary hypertension on postoperative clinical status and survival is unknown. A recent report has shown that residual pulmonary hypertension significantly compromised symptom status and functional capacity but did not appear to adversely affect medium-term survival [9].

A key question regarding the etiology of CTEPH is why pulmonary thromboemboli are stable and resistant to plasmatic anticoagulation. One mechanism may be an altered coagulation process, either inherited or acquired, or a combination of both [10]. However, this explanation is not sufficient because there are many patients without known coagulation problems. The other mechanism may be fibrinolysis-resistant fibrin clots from patients with CTEPH, when compared with fibrin clots from healthy control subjects [11]. A recent insight for the poor resolution of CTEPH indicates that modification of fibrinogen in

* Corresponding author at: Department of Respirology (B2), Graduate School of Medicine, Chiba University, 1-8-1 Inohana, Chuo-ku, Chiba 260-8670, Japan. Tel.: +81 43 222 7171x5471; fax: +81 43 226 2176.
*E-mail address:* miki-m@tg7.so-net.ne.jp (M. Maruoka).
[1] These authors contributed equally to this work.

0167-5273/$ – see front matter © 2011 Elsevier Ireland Ltd. All rights reserved.
doi:10.1016/j.ijcard.2011.02.037

CTEPH patients causes resistance of emboli to fibrinolysis [12,13]. These molecular alternations are paralleled by a resistance to thrombolysis [11]. However, this explanation is not sufficient because numerous genetic variants of human fibrinogen have been implicated in thrombotic diseases [14] and the resistance could be ascribed to, not only fibrinogen genetic polymorphisms, but also variances in post-translational modifications. An alternative mechanism may be *in situ* thrombosis in the lung initiated by a primary arteriopathy and/or endothelial dysfunction. However, it is unclear whether and how downstream *in situ* thrombosis could provoke proximal pulmonary artery thrombosis [1].

Chronic PH, including CTEPH, is characterized by obstructive intimal lesions, showing mainly a myofibroblastic phenotype and a variable degree of endothelial cell differentiation [15]. Of interest, non-resolving pulmonary thromboemboli in CTEPH have been shown to contain myofibroblasts [16].

Myofibroblasts are ubiquitous cells with characteristics of both fibroblasts and smooth muscle cells. They participate in wound healing and inflammatory response. They have the capacity to produce extracellular matrix (ECM) and, indeed, their excessive activation and inhibition of apoptosis may be the underlying process in many fibrotic diseases [17]. In addition, myofibroblasts being in the so-called stroma reaction of epithelial tumors may help the progression of cancer invasion [18].

We hypothesize that the unique microenvironment created by the unresolved clot may induce the formation of myofibroblasts with high growth potential in the clot, which may be an important mechanism in some parts of CTEPH patients.

The aim of this study has been to examine the characteristics of cell phenotypes in the organized thrombotic tissues of CTEPH. We isolated cells from the organized thrombotic tissues by PEA from patients with CTEPH and identified them as endothelial-like cells (EL) and myofibroblast-like cells (MFL). MFL were characterized as hyperproliferative, anchorage-independent, invasive and serum-independent.

We suggest that the formation of myofibroblasts with a high growth potential in the organized thrombotic tissues may be an important event in the pathobiology of this disease.

## 2. Materials and methods

### 2.1. Cell extraction

The PEA tissues and tissues outside these lesions of patients with CTEPH were obtained following PEA performed by Dr. Masuda at the Chiba Medical Center, Japan. Control pulmonary arteries are obtained following lung resection for peripheral cancer by Dr. Yoshino at the Chiba University Hospital, Japan. The PEA tissues were separated to two segments for isolation of cells: the intimal and the medial sides of the organized thrombotic material cut from regions surrounding the occlusion. The intimal side material, the medial side material, the neighbor tissue outside the thrombotic material which seemed to be the normal intima and control pulmonary arteries were minced using scalpels to remove some fresh thrombotic material found outside the endothelial layer and plated into a petri-dish (6 cm in diameter) coated with human fibronectin (BD Biosciences, San Diego, CA, USA). The explants were cultured in endothelial cell growth medium (EGM) supplemented with 5% fetal bovine serum (Lonza Inc, Allendale, NJ, USA) at 37° in a 5% $CO_2$ in air humidified incubator. Various explant outgrowth cells were dissociated and passaged free from surrounding cells using cloning cylinders (Millipore Corporate, Billerica, MA, USA).

The study was approved by the Research Ethics Committee of Chiba University School of Medicine, and all subjects gave their informed consent in writing.

### 2.2. Cell lines and reagents

Human pulmonary microvascular endothelial cells (HPMVEC) and normal human lung fibroblasts (NHLF) were obtained from Lonza Inc (Allendale, NJ, USA) and cultured using EGM and fibroblast growth medium (FGM) supplemented with 5% fetal bovine serum (Lonza Inc, Allendale, NJ, USA). HT1080 (fibrosarcoma cell line) and A549 (lung cancer cell line) were obtained from Takara biomedical (Othsu, Shiga, Japan) and cultured in RPMI-1640 medium supplemented with 5% fetal bovine serum (Lonza Inc, Allendale, NJ, USA). The following Ab were used: mouse anti-α-SM-actin (αSMA) Ab (1:1000, Sigma, St. Louis, MO, USA), mouse anti-vimentin Ab (1:200, DAKO, Carpinteria, CA, USA), mouse anti-human desmin Ab (1:100, DAKO, Carpinteria, CA, USA), mouse anti-human Ki-67 Ab (1:100, BD Biosciences Pharmingen, San Diego, CA, USA), anti-mouse IgG Ab conjugated with Rhodamine dye (1:500, Molecular Probes, Eugene, OR, USA), rabbit anti-von Willebrand factor (Factor VIII) Ab (1:1000, DAKO, Carpinteria, CA, USA), anti-rabbit IgG Ab conjugated with Alexa-488 fluorescent dye (1:500, Molecular Probes, Eugene, OR, USA). The Bromodeoxyuridine (BrdU) Flow Kit and the BD BioCoat™ FluoroBlok™ Invasion System (24-Multiwells) were from BD Biosciences (San Diego, CA, USA).

### 2.3. Immunofluorescence staining

Cells were fixed in a 1:1 mixture of methanol and acetone for 2 min followed by blocking with normal goat serum for 30 min, and incubated with primary antibodies (anti-α-SM-actin, Ab and anti-von Willebrand factor, anti-vimentin and anti-desmin Ab) for 1 h at room temperature and with secondary antibodies (anti-mouse IgG Ab conjugated with Alexa-594 fluorescent dye and anti-rabbit IgG Ab conjugated with Alexa-488 fluorescent dye) for 1 h at room temperature as described previously [19]. Stained cells were embedded in VectaShield mounting medium with DAPI (Vector Laboratories, Burlingame, CA, USA) and examined with a ZEISS Axioskop 2 microscope with the KS300 imaging system (Carl Zeiss, Inc, Thornwood, NY, USA). Positive cells were detected at 200× magnification using a fluorescence microscope.

### 2.4. BrdU-7-amino-actinomycin D binding assay

The rate of DNA synthesis was detected in cells by the Bromodeoxyuridine (BrdU) Flow Kit as described previously [20]. At passage 5 the cells were seeded at a density of $1.5 \times 10^4$ cells/cm$^2$ and were subcultured when they reached to 70–90% confluences (4–8 days). At these confluences cells were harvested and washed in cold PBS. During the final 8 h of culture, BrdU was added to dishes; cells were then fixed and permeabilized, and the DNA was denatured by treatment with fixative/denaturing solution. The detector fluorochrome-anti-BrdU monoclonal antibody (BD Bioscience Pharmingen) and 7-amino-actinomycin D (BD Bioscience Pharmingen), a fluorescent dye for labeling DNA, were then used for flow cytometric analysis. The cell-incorporated BrdU and total DNA content were analyzed using a flow cytometer.

### 2.5. Colony-forming assay

For colony-forming assay, cells at passage 5 were plated into 6-well flat-bottomed plates using a two-layer soft agar system with a total of $1 \times 10^4$ cells/well in a volume of 1.5 ml/well in the upper layer as described previously [21]. The underlayer contained 0.5% agar; the upper layer, 0.3% agar (BD Biosciences Pharmingen, San Diego, CA). The culture medium was EGM medium (Lonza Inc, Allendale, NJ, USA). For each plating experiment, 2× stock solutions of agar were prepared by autoclaving with distilled water and the agar was kept at 40 °C. For each layer, these stock solutions were mixed with prewarmed 2× EGM medium which concentration was achieved by Vivapore Concentrators (Vivascience Ltd, Stonehouse Glos, GL, UK) and 2 ml was carefully pipetted into each culture dish. This mixture became semisolid at room temperature within 20 min. Cultures were placed in a humidified atmosphere, 5% $CO_2$, at 37 °C. Visible colonies were scored after 14 days with an inverted microscope. All experiments were done at least three times using triplicate plates per experimental point.

### 2.6. Cell invasion and migration assay

Cell migration assays were conducted using BD BioCoat™ FluoroBlok™ Invasion System (24-Multiwell) as recommended by the manufacturer. For invasion assays through matrigel, $2.5 \times 10^4$ cells at passage 4 in the medium without serum were loaded in the top well of the chambers that contained BD Matrigel Basement Membrane Matrix over a polyethylene terephthalate membrane with 8-mm pores. Cells were allowed to invade for 16 h before the matrigel was removed, and invaded cells were fixed and stained with Calcein. Cells adhering to the bottom surface of the membrane were detected with a fluorescent plate reader.

### 2.7. Serum starvation

Cells at passage 4 were seeded at $1 \times 10^5$ in the 25 cm$^2$ flasks and were incubated with EGM without serum and the elements including growth factors and hormones for 3 weeks. At each indicated day, a flask was trypsinized and the cells were counted. The average values of 3 experiments were shown.

### 2.8. Statistical analysis

More than 3 independent experiments were subjected to statistical analysis. The results were expressed as mean ± SEM. Data were analyzed using Mann–Whitney's *U*-test, as appropriate. A $p<0.05$ was considered significant for all tests.

## 3. Results

### 3.1. The cellular composition of endarterectomized tissue in CTEPH

Two different cell types were isolated from the PEA tissues which were covered by endothelium, not from fresh thrombotic material which can be also found during PEA, in each of the 15 cases with CTEPH (Table 1) [22]. The cell types were determined by morphology as EL (rounded appearance and cell–cell contact of the monolayer) and MFL (spindle-shape with cytoplasmic extensions) (Fig. 1A).

One cell type was isolated from the neighbor tissue outside the thrombotic material which seemed to be the normal intima in case 10, defined by morphology as endothelial-like cells from the neighbor tissue (ELNT) (Fig. 1A). Moreover, the other cell type was isolated from the vessel wall adventitia of control pulmonary arteries, defined by morphology as fibroblast-like cells (PAFL). They are used as control cells prepared in the same way as the CTEPH specimens. Unfortunately, both endothelial-like and myofibroblast-like cells were not isolated from the vessel wall intima and media.

The cells outgrown from the organized thrombotic tissue, the neighbor tissue and control pulmonary arteries were further characterized by immunohistochemical staining for desmin, vimentin, anti-von Willebrand factor (Factor VIII) and anti-α-SM-actin (αSMA). EL and ELNT were positive for the endothelial cell (EC)-specific marker (Factor VIII) and the mesenchymal-specific marker (vimentin) and negative for the 2 smooth muscle cell (SMC)-specific markers (desmin and αSMA) (Fig. 1B). MFL were Factor VIII and desmin negative and vimentin and αSMA positive (Fig. 1B). PAFL were Factor VIII, desmin and αSMA negative and vimentin positive (data not shown).

### 3.2. Proliferative activity of MFL

MFL exhibited increased proliferative potential, grew without cell–cell contact inhibition and started piling up and forming foci in the culture dishes (6 cm in diameter) which were coated with human fibronectin (Fig. 2A). In order to confirm the proliferative activity, the number of proliferating cells was assessed by flow cytometry. Cells which have synthesized DNA can be identified by immunofluorescent staining of incorporated BrdU and flow cytometric analysis. BrdU, an analog of the DNA precursor thymidine, is incorporated into newly synthesized DNA by cells entering and progressing through the S (DNA synthesis) phase of the cell cycle. We found an increase in the number of BrdU positive cells in MFL, but no increase in the incorporation of BrdU by HPMVEC, NHLF, ELNT and PAFL (Fig. 2B).

**Table 1**
Clinical and haemodynamic data.

| | |
|---|---|
| Subjects | 15 |
| Gender | |
| Male/female | 6/9 |
| Age years | |
| Median (range) | 57.7 (38–71) |
| Haemodynamic data[a] | |
| Pra mm Hg | |
| Median (range) | 6.3 (1–19) |
| Mean Ppa mm Hg | |
| Median (range) | 49.7 (37–65) |
| CI l/min/m$^2$ | |
| Median (range) | 2.59 (1.46–4.75) |
| PVR dyn s cm$^{-5}$ | |
| Median (range) | 828.5 (421–1325) |
| $PaO_2$ Torr | |
| Median (range) | 60.2 (46.2–83.4) |
| $PVO_2$ Torr | |
| Median (range) | 32.4 (24.2–43.0) |
| Risk factors | |
| Previous VTE | 9 |
| Recurrent VTE | 4 |
| APA/LAC | 5 |
| Malignancy | 1 |
| Gastrointestinal carcinoma | 1 |
| Ventriculo-atrial shunt | 1 |
| Thyroid hormone replacement | 0 |
| Pacemaker | 0 |
| Infected pacemaker | 0 |
| Splenectomy | 0 |

*Definition of abbreviations*: Pra = right atrial pressure; mean Ppa = mean pulmonary arterial pressure; CI = cardiac index; PVR = pulmonary vascular resistance; PaO2 = arterial O2 pressure; PvO2 = mixed venous O2 pressure; VTE = venous thromboembolism; APA/LAC = antiphospholipid antibodies/lupus anticoagulant.

[a] At the time of pre operation.

### 3.3. Anchorage independent growth of MFL

Because MFL grew without cell–cell contact inhibition and started piling up and forming foci in the culture dishes, we examined the ability of these cells to form colonies in soft agar. MFL showed anchorage independence in soft agar colony assays (Fig. 3A). There was an increase in the number of colonies of MFL when compared with HPMVEC, NHLF, ELNT and PAFL (Fig. 3B).

### 3.4. Invasive and migratory activity of MFL

The ability of tumor cells to migrate and invade neighboring tissues is also a critical aspect of their metastatic potential [23,24]. When MFL and EL from endarterectomized tissue were co-cultured, MFL appeared to surround and invade the colonies of EL (Fig. 4A). Because of this cell behavior we assessed the invasion and migration activity of MFL. Using the BD BioCoat™ FluoroBlok™ Invasion assay, NHLF, ELNT, PAFL, the invasive fibrosarcoma cell line HT1080, the invasive lung cancer cell line A549 and MFL were allowed to invade for 16 h. MFL showed high invasive and migratory activity similar to HT1080 and A549 cells when compared with NHLF, ELNT and PAFL (Fig. 4B). From this data we concluded that, MFL shared *in vitro* an invasive potential with sarcoma and cancer cell lines.

### 3.5. Serum independent growth of MFL

In the absence of serum, HPMVEC stopped proliferating and rapidly underwent apoptotic death, likewise NHLF, ELNT and PAFL stopped proliferating and gradually became apoptotic (Fig. 5). In clear contrast, MFL survived indefinitely in the absence of serum, especially MFL from case 2, 5 and 12 kept proliferating (Fig. 5).

## 4. Discussion

Here we report the isolation and expansion in culture of cells from the PEA tissues which are covered by endothelium from patients with CTEPH. These cells were characterized by morphology and immunohistochemical staining as EL and MFL (Fig. 1A and B). EL tended to be isolated from the intimal side of the organized thrombotic material and MFL from the medial side material, however the latter could come from both. The total number of cultures was 16 and only one case failed because of an unknown reason. One of all the patients presented with gastrointestinal carcinoma, but not concurrent cancer (Table 1). However, there was no treatment interfering with growth of the isolated cell. Because at present it is not feasible to conduct *in vivo* studies in patients to characterize the thrombus/vessel wall interactions, we isolated cells from thrombus material in order to conduct *ex vivo* studies.

Hanahan and Weinberg in their landmark paper entitled "Hallmarks of Cancer" listed angiogenesis, evasion of apoptosis, self-sufficiency in growth signals, insensitivity to anti-growth signals and tissue invasion to characterize malignancy [25]. In our investigation MFL from endarterectomized tissue showed hyperproliferation (Fig. 2B), anchorage independence of growth (Fig. 3A and B), invasive capacity (Fig. 4B) and serum independence of growth (Fig. 5). All of

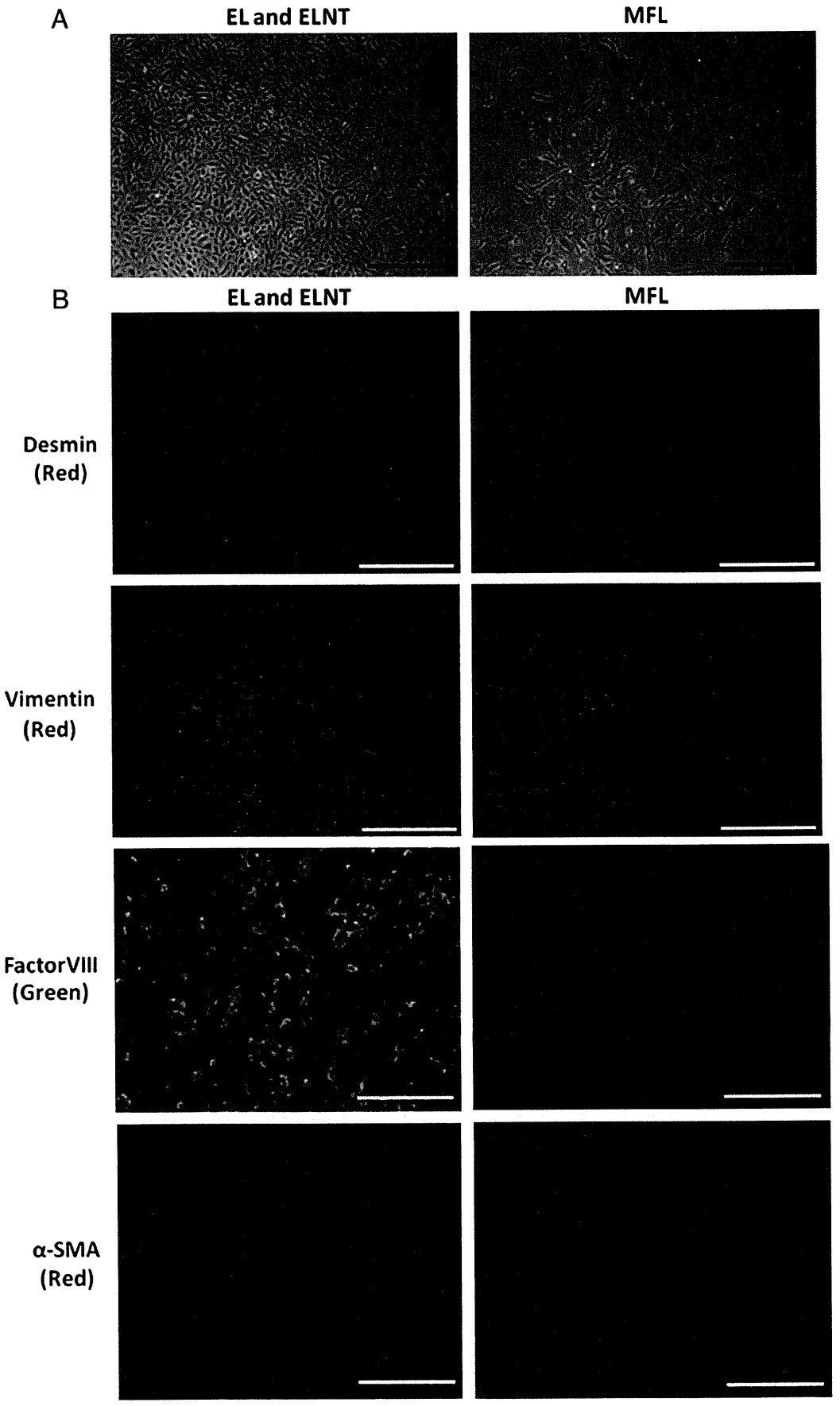
A
EL and ELNT
MFL
B
EL and ELNT
MFL
Desmin (Red)
Vimentin (Red)
FactorVIII (Green)
α-SMA (Red)

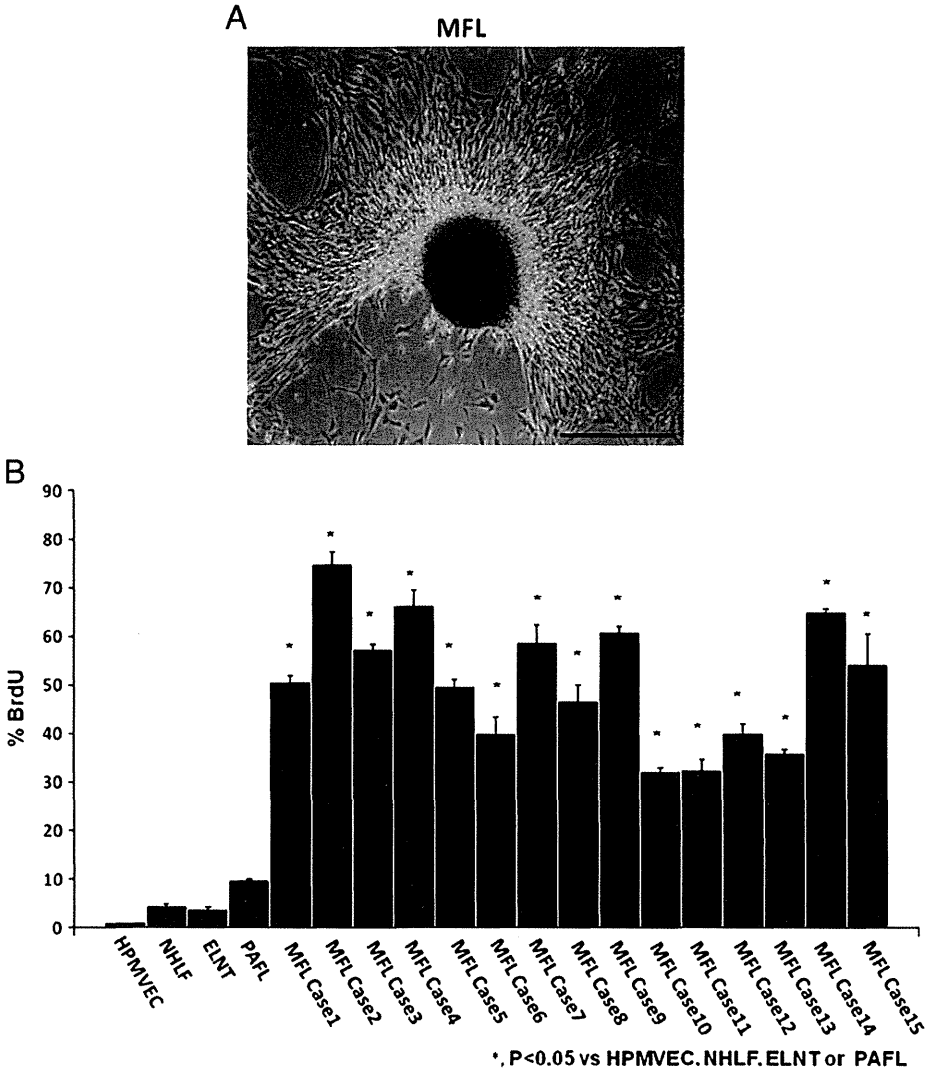


**Fig. 2.** BrdU-7-amino-actinomycin D binding assay. A) Light microscopy of MFL at 3rd passages. Magnification was 100×. Scale bar = 100 μm. B) Quantification of proliferating MFL at 4th passages. Individual cells that had synthesized DNA were determined by the immunofluorescent staining of incorporated bromodeoxyuridine (BrdU). The incorporated BrdU was stained with specific anti-BrdU fluorescent antibodies. The levels of cell-associated BrdU were measured by flow cytometry; error bars represent ± SD from experiments done in triplicate. *, $p<0.05$; $n>4$. *Definition of abbreviations*: HPMVEC = Human pulmonary microvascular endothelial cells; NHLF = Normal Human Lung Fibroblast; ELNT = endothelial-like cells from the neighbor tissue; MFL = myofibroblast-like cells; PAFL = pulmonary arterial fibroblast-like cells.

these traits displayed *in vitro* assays reflect cancer-defining mechanisms, raising the question whether the cells contained in the endarterectomized tissue of patients with CTEPH express a latent malignant potential. However, the absence of data on acquired capability, i.e., metastasis and sustained angiogenesis, thus reveals these cells to not be malignant neoplasms.

Generally after intimal injury and thrombus formation, fibroblasts differentiate into contractile and secretory myofibroblasts that contribute to tissue repair during wound healing. To terminate the process of intimal repair, the reconstructed ECM again takes over the mechanical load and myofibroblasts disappear by massive apoptosis [26]; thus stress release is a powerful promoter of myofibroblast apoptosis *in vivo* [27] (Fig. 6). Myofibroblasts, however, can severely impair organ function when contraction and ECM protein secretion become excessive, such as in lung fibrosis [28], liver fibrosis [29] and during the formation of atheromatous plaques and restenotic lesions [30,31]. We wondered whether hyperproliferative MFL in CTEPH could maintain *in situ* thrombosis in the lung that was resistant to thrombotic resolution resulting in non-resolving pulmonary thromboemboli (Fig. 6). However, there is no evidence to indicate that MFL alter coaguation/fibrinolysis in the patients of CTEPH. Indeed, it has been demonstrated the existence of putative endothelial progenitor cells in endarterectomized tissues of patients with CTEPH [32]. Moreover, Firth et al. have recently reported the presence of multipotent mesenchymal progenitor cells within endarterectomized tissues of patients with CTEPH [33]. These studies suggested that the unique microenvironment created by the stabilized clot may promote these progenitor cells to differentiate and enhance intimal remodeling [32,33].

**Fig. 1.** The cells from endarterectomized tissue. A) The 2 kinds of cells from endarterectomized tissue and the neighbor tissue were microscopically assessed. The magnification was 100×. Scale bar = 100 μm. B) The 2 kinds of cells from endarterectomized tissue and the neighbor tissue were assessed by immunofluorescent staining for anti-Desmin, anti-Vimentin, anti-Factor VIII and anti-α-SMA to confirm phenotypes of the cells. The blue staining was DAPI. Magnification was 200×. *Definition of abbreviations*: EL = endothelial-like cells; ELNT = endothelial-like cells from the neighbor tissue; MFL = myofibroblast-like cells. Scale bar = 50 μm.

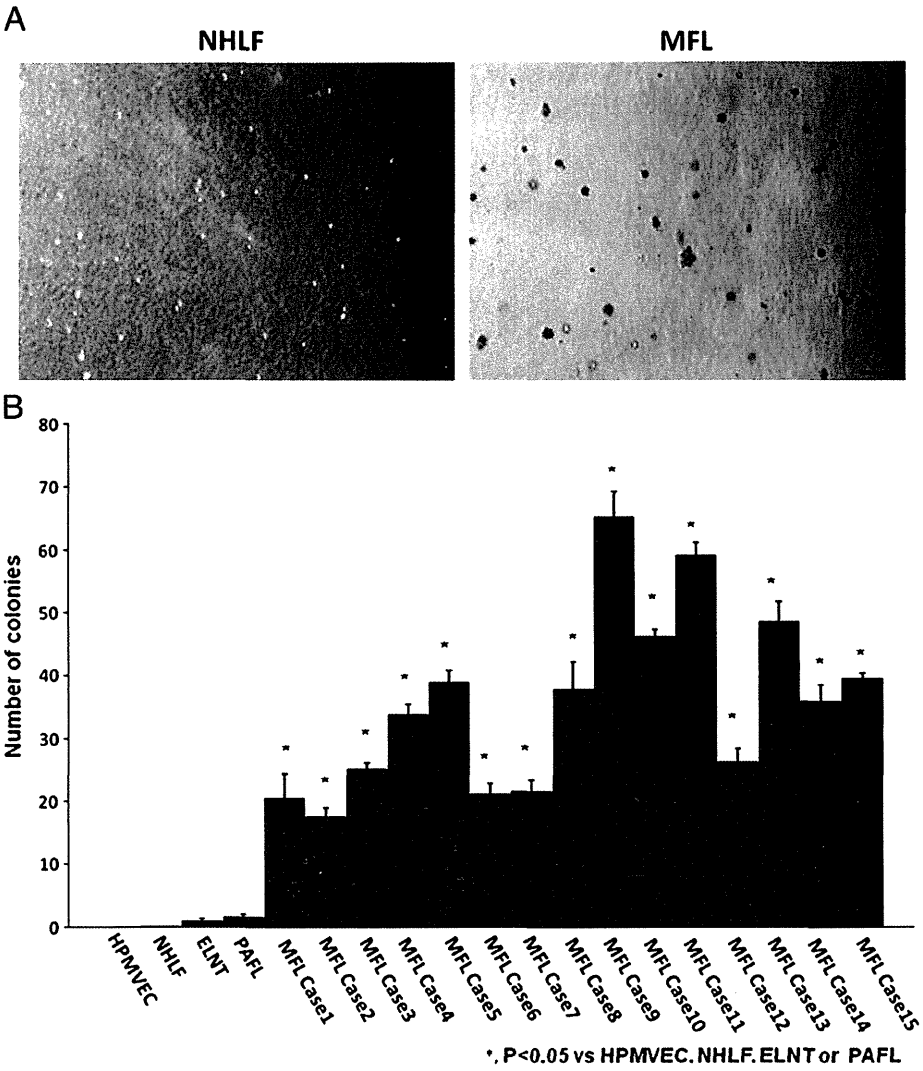


**Fig. 3.** Colony-forming assay. A) NHLF at 5th passages, MFL at 4th passages were trypsinized and replated on soft agar. Microphotographs showed colonies grown in soft agar for 2 weeks. Magnification was 40×. Scale bar = 100 μm. B) Numbers of colonies per microscopic field were counted; error bars represent ± SD from experiments done in triplicate. *, $p<0.05$. *Definition of abbreviations*: HPMVEC = Human pulmonary microvascular endothelial cells; NHLF = Normal Human Lung Fibroblast; ELNT = endothelial-like cells from the neighbor tissue; MFL = myofibroblast-like cells; PAFL = pulmonary arterial fibroblast-like cells.

Although the traditional view has been that acute pulmonary embolism is the initiating event, it remains unclear whether additional *in situ* thrombosis and small vessel disease are required for the progression to pulmonary hypertension which is observed in only about 3.8% of all patients with acute thromboembolic disease [6,34]. The identification of other than plasmatic problems of clot formation [22] has led to the concept that thromboembolic events in combination with infection, inflammation, autoimmunity or malignancy trigger an intravascular remodeling process that involves the thrombus itself as well as small resistance vessels [35]. Indeed, the patients in this study had the risk factors including malignancy and antiphospholipid antibodies/lupus anticoagulant (Table 1), indicating that these relationships are not put into doubt.

Theoretically, there exist large (elastic arteries) and small (muscularised arteries <0.5 mm of diameter) vessel diseases in CTEPH. The first is related to the obstructive lesions derived by unresolved emboli (or local thrombi) and the latter is considered a consequence of the hypertensive state and is virtually identical to those observed in pulmonary arterial hypertension (PAH) [6]. We wondered whether MFL could play a role in the small vessel disease in CTEPH. In *ex vivo* proof of principle experiments we have demonstrated that actively proliferating endothelial cells without evidence of apoptosis, via a mechanism of endothelial–mesenchymal transdifferentiation could perhaps contribute to the development of small vessel disease [19,20]. In this scenario, EC apoptosis resulted in the selection of an apoptosis-resistant, proliferating phenotypically altered EC phenotype. In CTEPH, especially in large vessels, we speculate that EC apoptosis after intimal injury might induce not only EC, but also SMC and/or fibroblast alteration and have led to the emergence of these very unique cell types that was shown in this study. Recently, high expression levels of platelet-derived growth factor (PDGF) and PDGF receptors in endarterectomized tissue of patients with CTEPH have been shown, suggesting the existence of hyperproliferative cells [36]. Moreover, fibroblasts with unique proliferative capabilities and loss of growth suppressive mechanisms induced by hypoxia have been previously described [37]. Rai et al. recently, in a contextual analysis and summarizing published data from several laboratories, proposed a paradigm shift in an attempt to explain the pathobiology of small vessel disease in severe PH as a quasi-neoplastic process [38,39].

In conclusion, we identified and characterized cell phenotypes in endarterectomized tissues of patients with CTEPH. MFL show cancer-

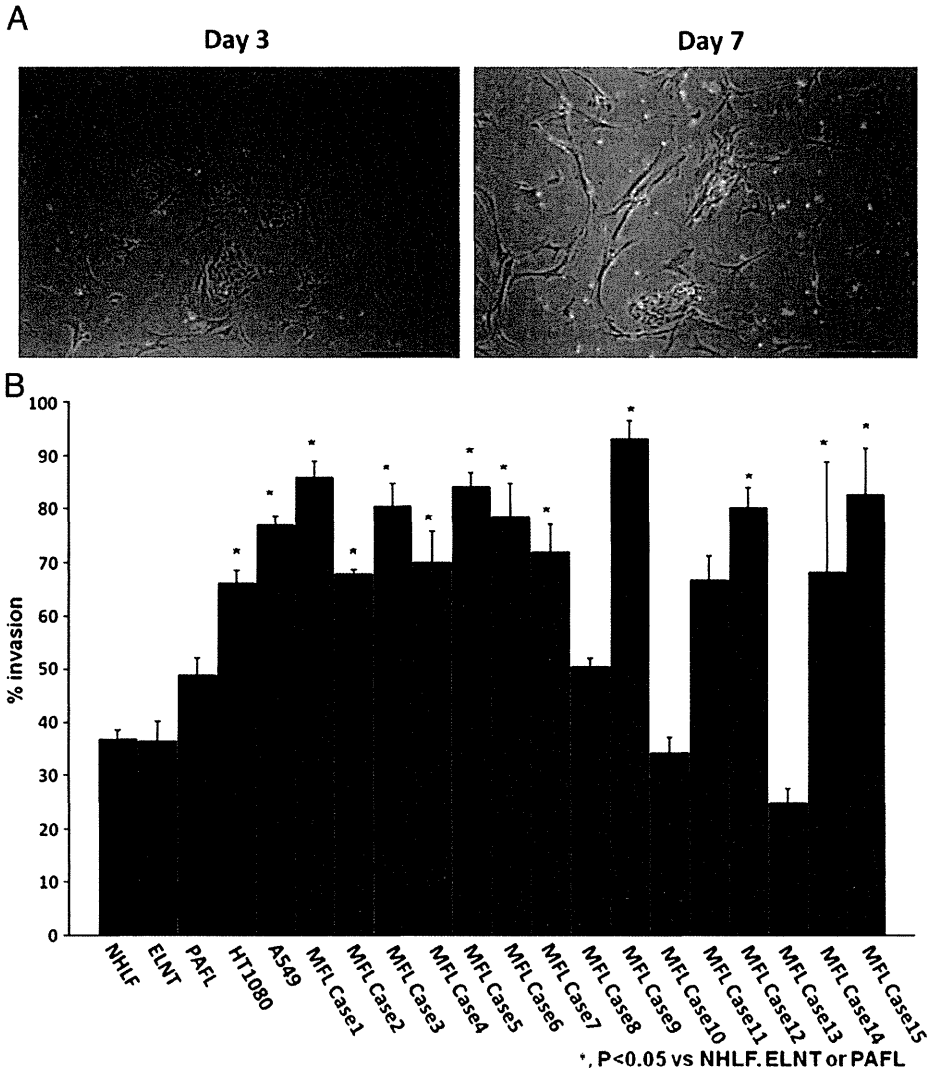


**Fig. 4.** Cell invasion and migration assay. A) Light microscopy of MFL and EL from endarterectomized tissue at 2nd passages. These cells were co-cultured. Magnification was 100×. Scale bar = 100 μm. B) Cell invasion and migration activity in MFL was determined. For the BD BioCoat™ FluoroBlok™ Invasion assay, NHLF, the invasive fibrosarcoma cell line HT1080, the invasive lung cancer cell line A549, PAFL and MFL were allowed to invade for 16 h; error bars represent ± SD from experiments done in triplicate. *, $p<0.05$; $n>4$. *Definition of abbreviations*: HPMVEC = Human pulmonary microvascular endothelial cells; NHLF = Normal Human Lung Fibroblast; EL = endothelial-like cells; ELNT = endothelial-like cells from the neighbor tissue; MFL = myofibroblast-like cells; PAFL = pulmonary arterial fibroblast-like cells.

like characteristics, i.e., hyperproliferation, anchorage-independent growth, invasive capacity, and serum independent growth, although the absence of data on acquired capability, specifically metastasis and sustained angiogenesis, reveal that these cells are not cancers [39]. It is possible that the microenvironment provided by the unresolved clot may stimulate this erroneous cell proliferation, although it is uncertain whether these myofibroblasts could be an important mechanism in some parts of CTEPH patients.

Whether- or by what mechanism these cells with an *in vitro* anchorage-independent and invasive potential contribute to the development of severe pulmonary hypertension caused by small and large vessel diseases remains speculative, since the appropriate control thrombotic material from patients with chronic pulmonary embolic disease, but without pulmonary hypertension, is not available for examination. Further, we fully realize the limitation of our data interpretation which is based on *in vitro* studies of cultured cells and that the existence of dysregulated myofibroblasts in CTEPH is not sufficient to address the hypothesis. Moreover, we acknowledge the purely descriptive nature of our work that does not confer any pathophysiological evidence in CTEPH. However, we believe that our data may be consistent with the concept that vascular embedded-cell dysfunction or disease of the large and small lung arteries is a critically important root cause of severe and progressive pulmonary hypertension. If indeed *in situ* thrombosis, rather than single or multiple bouts of embolism, is related to the development of CTEPH, then one would expect to find patients with the diagnosis of CTEPH without evidence of leg or pelvic vein thrombosis. Unfortunately data describing the presence or absence of leg or pelvic vein thrombosis in patients with CTEPH are frequently unavailable. Perhaps our data presented here, will stimulate investigations designed to support or disprove the concepts proposed in this communication. The injured endothelium and circulating tissue-factor bearing microparticle [40,41] are new avenues for investigation in regards to CTEPH.

## Acknowledgments

This study was supported by the Research Grants for the Respiratory Failure Research Group, the Cardiovascular Diseases (19–9), and the Research on Intractable Diseases (22–33) from the